Journal of Marine Research, 66, 87–126, 2008

Ocean color data assimilation with material conservation for improving model estimates of air-sea CO_2 flux

by John C. P. Hemmings[1], Rosa M. Barciela[2] and Michael J. Bell[2]

ABSTRACT

A nitrogen balancing scheme for ocean color data assimilation in general circulation models is described and its potential for improving air-sea CO_2 flux estimates is demonstrated. Given increments for phytoplankton, obtainable from a univariate surface chlorophyll analysis, the scheme determines mixed layer concentration increments for the other nitrogen pools: zooplankton, detritus and dissolved inorganic nitrogen (DIN). The fraction of the phytoplankton increment to be balanced by changing DIN varies dynamically with the likely contributions of phytoplankton growth and loss errors to the error in the background state. Further increments are applied below the mixed layer wherever positive DIN increments in shallower layers would otherwise cause the creation of unrealistic sub-surface minima. Total nitrogen at each grid point is conserved where possible.

The scheme is evaluated by 1-D twin experiments for two contrasting locations in the North Atlantic, in which synthetic chlorophyll observations are assimilated in an attempt to recover known system trajectories generated by perturbing model parameters. Dissolved inorganic carbon (DIC) and alkalinity tracers, controlled by the nitrogen dynamics, determine the biological modification of sea-water pCO_2 at the ocean surface. Assimilation affects DIC and alkalinity directly, the increments being inferred from the nitrogen increments, as well as having a post-analysis effect via the dynamics. It gives major improvements in surface pCO_2 at 50N but less improvement at 30N where errors in the phytoplankton nitrogen:chlorophyll ratio cause it to have a detrimental effect in summer. Beneficial effects of nitrogen balancing are demonstrated by comparison with experiments in which only phytoplankton and DIC are updated in the analysis.

1. Introduction

Changes in biogeochemical cycles in response to anthropogenic forcing of the global climate system have the potential to introduce strong climate feedbacks. However, system complexity prevents us making reliable predictions of the magnitude or even the sign of such feedbacks at present. Biological modification of the oceanic uptake of CO_2 and the vertical carbon flux within the ocean seems likely to play an important role and it is important to improve our understanding of the processes controlling these fluxes and how they might vary in the future. Ocean color data from satellites, now available as a continuous time-series

1. National Oceanography Centre, European Way, Southampton SO14 3ZH, United Kingdom. ***email: j.hemmings@noc.soton.ac.uk***

2. Met Office, FitzRoy Road, Exeter, EX1 3PB, United Kingdom.

with near global coverage since the launch of the Sea-viewing Wide Field-of-view Sensor (SeaWiFS) in 1997, provide a particularly important resource in this context because of their spatial and temporal coverage, unachievable with *in situ* measurements. However, the data relate almost exclusively to the near surface phytoplankton and must be combined with information about other components of the system to quantify net carbon fluxes. This necessitates assimilating the data into models of the global ocean that provide a synthesis of our understanding from theory and observation.

Present understanding of pelagic ecosystems has led to a number of ocean general circulation models (OGCMs) with explicit plankton sub-models, providing different representations of the global carbon cycle (e.g. Six and Maier-Reimer, 1996; Palmer and Totterdell, 2001; Aumont *et al.*, 2003; Gregg *et al.*, 2003; Moore *et al.*, 2004). The plankton models represent elemental cycles in terms of flow of material between compartments, each compartment representing a biotic or abiotic component of the system. The number of compartments varies between models. The degree of complexity desirable is dictated in part by the application but the amount that can be justified in the absence of appropriate observational constraints is also an issue (Anderson, 2005). Progress in quantifying important feedbacks will require the development of more accurate simulation systems in which models are constrained by earth observation data from satellite and *in situ* measurements. Sequential data assimilation procedures are needed that combine information from simulations and observations to provide optimal estimates of the ocean state. In addition, because biogeochemical models are necessarily empirical, with many constant parameters representing factors that in nature are highly variable, data assimilation has an important role to play in improving the models themselves by constraining the values of these parameters. Parameter estimation techniques are valuable, not only for improving individual models, but also for allowing different models of varying complexity to be objectively evaluated against each other in the presence of parameter uncertainty (Friedrichs *et al.*, 2006).

Most data assimilation work in the biogeochemical modeling field to date has focussed on parameter estimation using inverse methods. These require a large number of model integrations, which has restricted their application to 0-D or 1-D models or short period integrations of 3-D models of limited spatial extent or resolution. Studies are typically based on *in situ* data sets from individual time-series sites (Matear, 1995; Fasham and Evans, 1995; Prunet *et al.*, 1996a,b; Hurtt and Armstrong, 1996; Spitz *et al.*, 1998, 2001; Fasham *et al.*, 1999, 2006; Fennel *et al.*, 2001; Schartau *et al.*, 2001; Friedrichs, 2002; Faugeras *et al.*, 2003, 2004; Dadou *et al.*, 2004; Kuroda and Kishi, 2004; Weber *et al.*, 2005). Calibrated models are rarely tested at other sites so it is unclear how widely applicable the resulting parameter sets might be. Recent North Atlantic studies have started to address this problem by optimizing over multiple time-series sites in different parts of the basin simultaneously (Hurtt and Armstrong, 1999; Schartau and Oschlies, 2003a,b). Oschlies and Schartau obtained promising results from a basin-scale validation of a 3-D model calibrated in 1-D mode with data from 3 different sites. However, model-data misfits remained much larger than the observational error estimates.

The need for globally applicable models and the sparse nature of *in situ* measurements makes the use of satellite data in model calibration highly desirable, ideally in combination with data from multiple time-series sites. Some recent studies using satellite ocean color data have explored how optimal model parameters might vary spatially. Garcia-Gorriz *et al.* (2003) calibrated a 3-D model of the Adriatic Sea to fit SeaWiFS chlorophyll data and found differences between optimal parameters for northern and southern regions. In a similar study, in the Bay of Biscay, Huret *et al.* (2007) also found differences in parameter values between different study areas. Tjiputura *et al.* (2007) assimilated seasonal maps of SeaWiFS chlorophyll into a coarse resolution model of the global ocean, performing separate calibrations for each season. When the domain was divided, assimilation of data for different latitude regions produced different results, with assimilation of high latitude data producing greater variance in parameter values between seasons than tropical data. Other studies using 0-D models have optimized parameters for the whole annual cycle. Hemmings *et al.* (2003) assimilated SeaWiFS chlorophyll data and *in situ* estimates of winter-time nitrate at points on a 5° grid in the North Atlantic, testing their results against unassimilated data at alternate grid points. They found that regional calibrations gave a better fit to the validation data than that given by the optimal parameter set for the whole domain. Hemmings *et al.* (2004) introduced an objective method for finding the number and geographic scope of parameter sets that would allow the best fit to be achieved. Losa *et al.* (2004) investigated spatial variation in optimal model parameters by assimilating chlorophyll data at individual points on a similar grid using a weak constraint technique that allows for model error. Introducing the resulting parameter variations into a 3-D simulation greatly improved the representation of regional scale chlorophyll patterns (Losa *et al.* 2006). Together, these studies suggest that any attempt to calibrate present models for the global ocean invites the prospect of obtaining parameter sets that are a poor compromise for all locations. Allowing spatial variation in parameter values might be a useful way of learning about model deficiencies with a view to developing more general parameterizations.

Although the inherent uncertainties associated with plankton models have encouraged the use of biogeochemical data for parameter estimation rather than state estimation, there has been some progress with sequential state estimation techniques too (Armstrong *et al.*, 1995; Anderson *et al.*, 2000; Popova *et al.*, 200a,b; Allen *et al.*, 2003; Beşiktepe *et al.*, 2003; Hoteit *et al.*, 2003; Losa *et al.*, 2003; Natvik and Evensen, 2003; Magri *et al.*, 2005; Dowd, 2006; Torres *et al.*, 2006; Raick *et al.*, 2007; Gregg, 2007; Lenartz *et al.*, 2007). One of these, a property-conserving Monte Carlo method known as the Sequential Importance Resampling filter, has been used to estimate parameters concurrently with the model state (Losa *et al.*, 2003; Dowd, 2006). In this case, the parameters are not constrained to be invariant in time. Seasonal cycles of parameter values derived from long hindcasts with the SIR filter could potentially replace fixed parameters in operational models (Brasseur *et al.*, 2005). Alternatively, the parameter time series might suggest improved parameterizations of the ecosystem response to seasonal change in the physical environment.

The spatial coverage provided by satellite data makes them particularly well suited to sequential state estimation schemes in 3-D circulation models. In early work by Ishizaka (1990), chlorophyll data from the early Coastal Zone Color Scanner (CZCS) sensor were used to re-initialize the phytoplankton field in an embedded NPZD model of the nitrogen cycle. This is a type of model with 4 nitrogen compartments representing dissolved inorganic nitrogen (DIN), phytoplankton, herbivorous zooplankton and detritus. Nitrogen, as a limiting nutrient for phytoplankton growth, is one of the most important factors controlling the carbon cycle. The analysis was multivariate, the other nitrogen variables being updated to satisfy a temperature based total nitrogen criterion. Only one chlorophyll map was assimilated and the simulation state was found to revert to that of the free running model within 2 days.

In the first truly sequential assimilation of satellite chlorophyll, Armstrong *et al.* (1995) used a nudging scheme to assimilate CZCS chlorophyll data into a 7 compartment nitrogen cycle model of the North Atlantic. Here, the analysis was univariate. Instability in one of the unassimilated variables led to unsatisfactory results with the 7 compartment model but experiments with a more complex 'multi-food chain' version showed more promising results. Natvik and Evensen (2003) used an ensemble Kalman filter (EnKF) to assimilate SeaWiFS chlorophyll data into a similar North Atlantic model. The EnKF is appropriate for biogeochemical models because of its effectiveness in simulating the evolution of multivariate error statistics in non-linear systems. However, the number of ensemble members required in the simulation makes it computationally expensive. Multivariate assimilation of chlorophyll allowed the system to produce a pattern of spring bloom development over the basin that was consistent with the data. Gregg (2007) assimilated daily SeaWiFS data into a model of the global ocean with 8 nitrogen compartments, 4 of which represented different phytoplankton functional types. A simple univariate scheme, the Conditional Relaxation Analysis Method (CRAM), was used and the resulting chlorophyll increments were partitioned between the phytoplankton types in the analysis, retaining their relative concentrations. Model chlorophyll was validated against satellite and *in situ* chlorophyll data. In addition, primary production was validated against alternative estimates derived directly from satellite data. Results for chlorophyll were greatly improved over the free run and production was also improved but to a lesser extent. Nerger and Gregg (2007a) performed a similar univariate experiment with a simplified version of the SEIK filter as a step towards a multivariate assimilation system. The SEIK filter is an efficient ensemble-based Kalman filter that uses a low rank approximation of the covariance matrix to describe the state error characteristics. Static error statistics were used in this implementation. Nevertheless, a small improvement in performance over the bias correction method was obtained for surface chlorophyll. Further improvement was achieved with the addition of an online bias correction method (Nerger and Gregg, 2007b). Unassimilated variables were not validated against independent observations in any of these studies so the benefits of chlorophyll assimilation with respect to other components of the system remain unclear.

Our focus in the present work is on estimating the air-sea flux of CO_2, driven by the pCO_2 difference across the air-sea interface. The primary aim of assimilating ocean color

is therefore to improve estimates of the seawater pCO_2. The biological controls on surface pCO_2 result from biotic modification of the total dissolved organic carbon (DIC) and the alkalinity by a combination of photosynthesis, respiration and calcification. In this context, an ocean color assimilation scheme must make the best possible use of phytoplankton-related information for correcting not just the phytoplankton biomass but all components of the system affecting DIC and/or alkalinity.

We present here a computationally efficient scheme for balancing daily surface phytoplankton increments in an NPZD nitrogen cycle model. The phytoplankton increments can be derived directly from univariate analyses of surface chlorophyll performed by existing sequential assimilation schemes. Its potential for improving surface pCO_2 estimates is evaluated by identical twin experiments in a 1-D test-bed. The design of the scheme is described in Section 2 and the evaluation experiments are described in Section 3. The results are then presented and the scheme's potential discussed.

2. The nitrogen balancing scheme

a. Principles

The nitrogen balancing scheme takes daily surface phytoplankton increments and determines surface increments for DIN, zooplankton and detritus and sub-surface increments for all four nitrogen tracers. The nitrogen increments are added to the existing or *background* state to obtain an *analysis* state which provides the initial conditions for the next 24 h of the simulation. The scheme is designed to correct for model error arising from inadequate representation of biological processes that transfer nitrogen between the four nitrogen compartments. While errors in physical transport processes will also have a strong effect on surface phytoplankton concentration, via their effects on the availability of DIN and light and the redistribution of biomass, it is inappropriate for a biogeochemical assimilation scheme to attempt to compensate for these effects. They should ideally be addressed by improving the physical simulation and are not considered in the design of the scheme presented here. In addition, there is no explicit treatment of errors in biogeochemical processes affecting the sinking rate of particles or errors in biological transport processes. In most models these are errors of omission: detritus is given a constant sinking velocity and plankton are treated as passive tracers. The importance of such errors, relative to errors in the inter-compartmental fluxes, will be model-dependent and is difficult to quantify at present, so their potential impact on the scheme's performance is unclear.

In the absence of gravitational sinking and biological transport, an ideal material conserving circulation model with perfect representation of advection and diffusion would introduce no errors in the distribution of total nitrogen, irrespective of errors in the partitioning of material between compartments. On this basis, balancing increments are made in such a way that the analysis conserves total nitrogen at each grid point if possible. Gravitational sinking and biological transport do not affect all nitrogen pools equally and, even if accurately represented, will interact with errors in partitioning between compartments to

cause errors in the total nitrogen field. The scheme cannot directly correct for such errors but aims to reduce them by making frequent corrections to the individual tracers.

The scheme uses two different local balancing models to calculate the required increments at individual grid points. In the upper mixed layer and below, down to its maximum depth over the last 24 hours, a local balancing model for phytoplankton increments is used to calculate increments for the other tracers. Below the current mixed layer, the situation is more complicated. Balancing increments made to surface DIN concentration sometimes leave behind unrealistic sub-surface DIN minima. Sub-surface DIN increments are then required to correct the profile, which introduces the need for a second local balancing model that responds to DIN increments instead of phytoplankton increments.

b. Increments to nitrogen tracers in the upper mixed layer

i. Overview. The nitrogen balancing model for phytoplankton increments calculates a time varying factor for each of the other tracers, referred to as a balancing factor, that sets the magnitude of its surface layer increment relative to that for phytoplankton. The absolute surface increments for DIN, zooplankton and detritus are

$$\Delta N = -b_{\mathrm{N}} \Delta P \tag{1}$$

$$\Delta Z = -b_{\mathrm{Z}} \Delta P \tag{2}$$

$$\Delta D = -b_{\mathrm{D}} \Delta P, \tag{3}$$

where b_{N}, b_{Z} and b_{D} are the calculated balancing factors for each tracer. The negated balancing factors can be interpreted as estimates of the ratio of the background error covariances to the phytoplankton background error variance. Importantly though, the balancing factors are not independent of the background state. For nitrogen conservation

$$b_{\mathrm{N}} + b_{\mathrm{Z}} + b_{\mathrm{D}} = 1. \tag{4}$$

Eq. 4 is satisfied by the balancing factor model, subject to the availability of nitrogen at the model grid point.

Material conservation provides a valuable constraint on the analysis but the issue of how best to partition the balancing increments remains. The optimal solution depends on the extent to which different processes contribute to the net phytoplankton error introduced since the last analysis. The time evolution of the phytoplankton concentration is given by

$$\frac{dP}{dt} = (G^{\bullet} - L^{\bullet})P + \text{ transport} \tag{5}$$

where $G^{\bullet}$ is the phytoplankton specific growth rate and $L^{\bullet}$ is the phytoplankton specific loss rate. Ignoring the effect of errors in transport, the phytoplankton error is caused by a combination of errors in growth and loss. Over a 24 h period, growth involves primarily the transfer of nitrogen between DIN and phytoplankton. A fraction of the nitrogen required

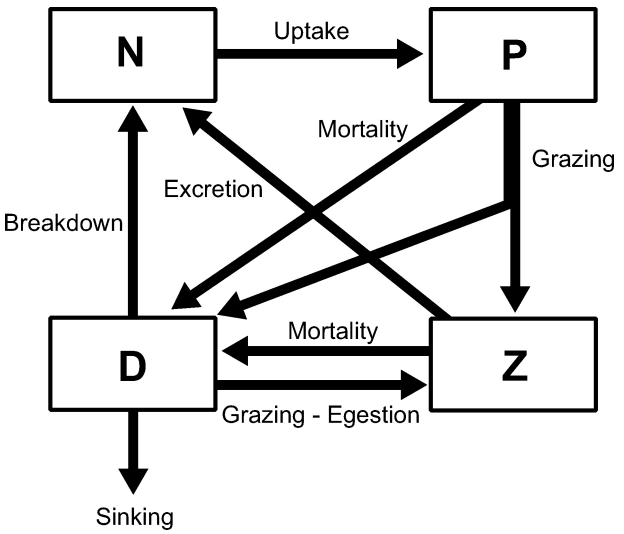

Figure 1. Intercompartmental nitrogen flows in an NPZD model. The compartments representing separate nitrogen pools are dissolved inorganic nitrogen (N), phytoplankton (P), herbivorous zooplankton (Z) and detritus (D). While there are differences between different NPZD models, the flows shown here indicate the dominant pathways. Some models do not include zooplankton grazing on detritus (e.g. Schartau and Oschlies, 2003a). Phytoplankton growth is accompanied by an uptake of DIN. Phytoplankton losses are dominated by grazing and mortality, a fraction of grazing being egested as detritus. A small loss direct to DIN due to exudation may be included (not shown). In a 24 h period, a relatively small fraction of the nitrogen lost due to grazing and mortality is returned to DIN either directly (fluxes not shown) or via zooplankton excretion and detrital breakdown.

for growth does originate from zooplankton and detritus but this only becomes significant when DIN is low. In contrast, loss effects are dominated by the transfer of nitrogen between phytoplankton and the combined zooplankton and detritus pools, a much smaller fraction being transferred to DIN. (The inter-compartmental flows are shown in Figure 1.) Partitioning of error variance is likely to reflect the amount of nitrogen transferred by each process so, in general, DIN errors will tend to be negatively correlated with phytoplankton error caused by errors in the growth rate, while errors in zooplankton and detritus will tend to be negatively correlated with phytoplankton error caused by errors in the loss rate.

The examples in Figure 2 show relative nitrogen errors in two different cases. In the first case, growth rate errors dominate so the positive phytoplankton error is associated with a negative error in DIN. In addition, smaller positive errors occur in zooplankton and detritus. This is because the excess concentration of phytoplankon increases the turnover of nitrogen from DIN to zooplankton and detritus via phytoplankton (i.e. the part of flux $G^\bullet P$ balanced by $L^\bullet P$ such that P is unaffected). The extent to which this occurs varies, depending on the phytoplankton specific turnover rate $T^\bullet = \min(G^\bullet, L^\bullet)$. In the second case, loss rate

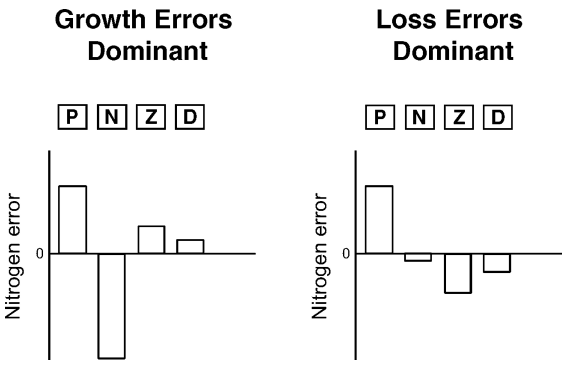

Figure 2. An example of relative errors in DIN (N), zooplankton (Z) and detritus (D) for the same error in phytoplankton (P) under different conditions. (See text for details.)

errors dominate and the same phytoplankton error, now attributable to insufficient loss, is associated primarily with negative errors in zooplankton and detritus with a small negative error in DIN. Turnover associated with the excess phytoplankton acts to increase the size of the DIN error and reduce the sizes of the zooplankton and detritus errors.

The variable inputs to the nitrogen balancing model are the model phytoplankton growth and loss rates, the nitrogen tracer concentrations and the phytoplankton error estimate $-\Delta P$. It uses a two phase approach to calculate the required balancing factors. Initial approximations, referred to as pre-adjustment factors, are first determined using information about the simulation since the last analysis together with the phytoplankton error information. Then, in the second phase, the balancing factor estimates are adjusted, taking into account the current background state, to satisfy a number of restrictions. The adjustment phase is important because of the large uncertainty associated with the initial estimates.

ii. Phase 1: pre-adjustment balancing factor determination. In the first phase, the value of the DIN balancing factor b_N is determined directly from the time-varying data. The sum of the zooplankton and detritus balancing factors $b_Z + b_D$ is $1 - b_N$, from the conservation equation (Eq. 4), and the relative magnitudes of b_Z and b_D are fixed by a parameter f_Z such that

$$b_Z = f_Z(1 - b_N) \tag{6}$$

and

$$b_D = (1 - f_Z)(1 - b_N). \tag{7}$$

f_Z is referred to as the zooplankton error fraction. Of the model error in the phytoplankton nitrogen lost to the combined zooplankton and detritus pools and remaining therein at the end of the 24 h period since the previous analysis, it indicates the fraction expected to contribute to zooplankton error. f_Z is prescribed as an external parameter (i.e. a parameter specified *a priori* as an input to the assimilation system).

For the purposes of deriving the initial value for b_N, the phytoplankton error estimate $-\Delta P$ is expressed as the sum of an error component x attributed to errors in the phytoplankton growth rate and an error component y attributed to errors in the phytoplankton loss rate. A model for b_N in terms of the unknown x and y is given by a function B, referred to as the DIN balancing function. $B(x, y)$ is defined in Appendix A (Eq. 20). It has a minimum value prescribed by an external parameter B_{MIN}. B_{MIN} indicates the fraction of the total phytoplankton loss error expected to contribute to DIN error. This is referred to as the DIN error fraction. (The zooplankton error fraction defined above is a fraction of the remaining error.) B also includes a time-varying turnover term dependent on the model phytoplankton specific growth and loss rates, denoted $G_0^\bullet$ and $L_0^\bullet$ respectively, and the model phytoplankton concentration P_0. The model values are those for the surface mixed layer, averaged over the 24 h assimilation time step. They are taken to be zeroth-order estimates of the true quantities. The unknown error components x and y are treated as particular values of two random variables X and Y, the joint distribution of which is modeled as a time-varying probability density function $p(x, y)$. Like the turnover term in B, $p(x, y)$ is dependent on $G_0^\bullet$, $L_0^\bullet$ and P_0. Details are given in Appendix A.

The pre-adjustment DIN balancing factor is set to the expected value of B, conditional on the estimated phytoplankton error:

$$b_N = E\left\{B\left(X, Y, P_0, G_0^\bullet, L_0^\bullet\right) \mid X + Y = -\Delta P\right\}, \tag{8}$$

where E is the expectation operator. For particular values of P_0, $G_0^\bullet$ and $L_0^\bullet$, b_N can be interpreted geometrically as a weighted average of $B(x, y)$ along the line $y = -(x + \Delta P)$ in the 2-D error component space, with the weighting function given by the estimated joint probability density $p(x, y)$. The reason for the dependence of b_N on the phytoplankton error becomes obvious if we consider, for example, the situation where the model phytoplankton growth rate is zero. A positive error, in this case, cannot be due to excessive growth and must therefore be wholly due to insufficient loss, whereas a negative error could be due to errors in growth or loss. Clearly, different balancing factors are appropriate for positive and negative phytoplankton errors.

iii. Phase 2: balancing factor adjustment. The balancing factor adjustment phase ensures that state-dependent restrictions on the size of the balancing increments are strictly enforced, while attempting to conserve nitrogen if possible. The restrictions are controlled by external parameter values. Firstly, to avoid excessive perturbation of the phytoplankton specific growth rate, DIN increments are not allowed to change the DIN limitation factor controlling growth rate in the model by more than a specified amount, relative to the value associated with the background state. In addition, zooplankton concentration cannot be changed by more than a specified amount, relative to the background concentration and detritus cannot be reduced below zero.

Adjustment of the balancing factors to satisfy the restrictions is carried out in a sequence of steps as follows. (1) If the background DIN is too low to allow the increment implied by

the pre-adjustment value of b_N to proceed, b_N is reduced. b_Z and b_D are then calculated from Eqs. 6 and 7 using the new value. (2) If the background zooplankton is too low to allow the implied zooplankton increment to proceed, b_Z is then reduced to transfer the excess zooplankton increment to detritus, b_D being increased accordingly to satisfy Eq. 4. (3) If, at this stage, there is insufficient detritus to satisfy a required negative increment, b_D must be reduced, transferring the excess to the combined zooplankton and DIN pools. In an attempt to contain the adjustment within the combined zooplankton and detritus pools, the excess is passed to zooplankton in preference to DIN by increasing b_Z if there is still scope for zooplankton adjustment. (4) Any remaining component of a negative detritus increment is transferred to DIN by increasing b_N instead, subject to the DIN restriction. If the restriction must be imposed at this stage, Eq. 4 cannot be satisfied and nitrogen is not conserved.

The DIN restriction is particularly important. The parameterization of the DIN limitation factor is model-specific but, in general, it increases rapidly with increasing DIN at low concentrations and saturates as DIN becomes plentiful. Basing the restriction on the limitation factor rather than the DIN concentration *per se* means that it only has a significant impact at low concentrations. Under such conditions, the recycling of organic nitrogen becomes important for growth causing the negative correlation between errors in phytoplankton and DIN to break down, so large DIN balancing increments are inappropriate. Critically, in fact, they will tend to cause undesirable positive feedback by increasing the magnitude of the growth rate errors. The DIN restriction compensates for the absence of a DIN dependent term in the DIN balancing function B.

The zooplankton restriction forces a transfer of increment from zooplankton to detritus when low zooplankton concentrations occur in combination with relatively large phytoplankton errors. This is consistent with the expectation that mortality, rather than grazing, is likely to be the dominant loss process when zooplankton concentration is low. The restriction compensates for the absence of a zooplankton dependency in f_Z.

c. Increments to nitrogen tracers below the upper mixed layer

The surface layer increments are applied down to the current mixed layer depth. Below this depth, compound increments for each tracer are possible. These are the sum of primary and secondary partial increments. The primary increments are based on the surface increments and are calculated using the phytoplankton-driven local balancing model described in Section 2*b*. They extend the analysis updates down to the maximum depth of the mixed layer in the last 24 hour assimilation time step, reducing the sensitivity of the vertically integrated biomass changes to the phase of the diel cycle at which the analysis occurs. The secondary increments are the DIN profile correction increments, together with balancing increments to the other tracers calculated by the DIN-driven local balancing model, described below. The basis for the secondary increments is the expectation that DIN concentrations increase monotonically with depth throughout most of the ocean, due to light limitation of photosynthetic uptake. They are required only in the event that the surface-layer and primary

increments alone would create an unrealistic sub-surface DIN minimum. The potential for this exists whenever there are positive DIN increments in shallower layers.

i. Primary increments. The primary phytoplankton increment is the surface increment scaled to the local background phytoplankton concentration so that the relative increment is constant with depth, subject to the restriction that the size of the increments must decrease monotonically with depth. The restriction avoids inappropriate updates to deep phytoplankton maxima where the phytoplankton error is unlikely to be positively correlated with that for the surface layer. Balancing increments for the other nitrogen tracers are based on the pre-adjustment balancing factors applied at the surface. These are adjusted to satisfy the restrictions described in Section 2*b* in the context of the sub-surface concentrations.

ii. Secondary increments. Non-zero secondary increments occur whenever the DIN concentration, after the addition of any primary increment, is still less than the analysis concentration for the level above, subject to the constraint that the total DIN increment must decrease monotonically with depth. The constraint protects against inappropriate updates to pre-existing sub-surface minima which could be due to the presence of different water masses below the surface.

A set of secondary increments at a model grid point consists of a positive DIN increment $\Delta_2 N$ plus negative balancing increments for the organic nitrogen tracers required for nitrogen conservation. The low sub-surface DIN is assumed to reflect uncorrected errors due to excessive DIN uptake by the model phytoplankton. However, it is not assumed that all of the missing nitrogen has remained in the phytoplankton pool. The fraction will depend on the phytoplankton loss rate in the model. Appropriate balancing increments are therefore determined for phytoplankton, zooplankton and detritus on the basis of the loss rate, taking into account the tracer concentrations.

The balancing increments are:

$$\Delta_2 P = -b_{2\mathrm{P}} \Delta_2 N \tag{9}$$

$$\Delta_2 Z = -b_{2\mathrm{Z}} \Delta_2 N \tag{10}$$

$$\Delta_2 D = -b_{2\mathrm{D}} \Delta_2 N, \tag{11}$$

where balancing factors $b_{2\mathrm{P}}$, $b_{2\mathrm{Z}}$ and $b_{2\mathrm{D}}$ are the balancing model's negated estimates for the ratios of the background error covariances for phytoplankton, zooplankton and detritus, to the DIN background error variance. Nitrogen is conserved where possible by attempting to satisfy the equation

$$b_{2\mathrm{P}} + b_{2\mathrm{Z}} + b_{2\mathrm{D}} = 1. \tag{12}$$

As in the phytoplankton-driven balancing model, a two-phase approach is used. In the first phase, the pre-adjustment value of the phytoplankton balancing factor is given by

$$b_{2\mathrm{P}} = \frac{1}{1 + 0.5\Delta t (1 - B_{\mathrm{MIN}}) L_0^{\bullet}}. \tag{13}$$

where Δt is the assimilation time step (24 h). The second term in the denominator is the estimated amount of the excess uptake $\Delta_2 N$ lost to zooplankton and detritus, expressed as a fraction of that remaining as phytoplankton $\Delta_2 P$. This loss is taken to be proportional to the mean phytoplankton error over the assimilation time step, estimated at $-0.5\Delta_2 P$. A fraction B_{MIN} of the loss is assumed to return to DIN over the period Δt. For levels below the deepest into which the surface mixed layer penetrated over the assimilation time-step, the 24 h average mixed layer loss rate $L_0^{\bullet}$ is replaced by the current loss rate determined from the background state. The balancing factors for zooplankton and detritus are:

$$b_{2\mathrm{Z}} = f_{\mathrm{Z}}(1 - b_{2\mathrm{P}}) \tag{14}$$

and

$$b_{2\mathrm{D}} = (1 - f_{\mathrm{Z}})(1 - b_{2\mathrm{P}}). \tag{15}$$

In the adjustment phase, the values for the balancing factors are adjusted to satisfy the restrictions on zooplankton and detritus reduction and a further restriction that the phytoplankton cannot be reduced by more than a specified factor by the secondary increment. The maximum reduction factor for phytoplankton applies to the size of the secondary increment relative to the intermediate concentration, i.e. the concentration present after any primary increment has been applied. This is in contrast to the zooplankton maximum reduction factor, which is a constraint for the whole analysis and applies to the total increment relative to the background concentration. Adjustment of the balancing factors is carried out using rules analogous to those described in Section 2*b*.

d. Summary

In summary, the steps in the balancing procedure at each point on the horizontal grid are as follows.

- Determine surface increments for DIN, zooplankton and detritus using the phytoplankton-driven local balancing model.
- Assign surface increments to each level above the mixed layer depth.
- For each layer below the mixed layer depth (until done), assign compound increments equal to the sum of any primary and secondary increments calculated as follows.

Primary increments, above maximum mixed layer depth only:

- Determine phytoplankton increment to match relative increment at surface, subject to the constraint that increment decreases with depth.
- Determine increments for DIN, zooplankton and detritus using the phytoplankton-driven local balancing model.

Secondary increments, where DIN concentration after the primary increment (if any) is less than in the layer above:

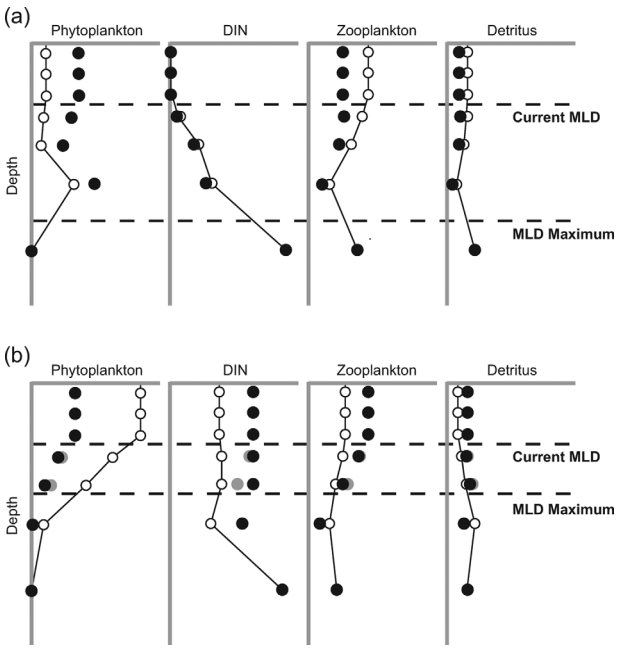

Figure 3. Two example analyses (a and b) showing the background state (open circles, joined), analysis state (black) and the tracer values corresponding to primary increments only (grey). The current mixed layer depth and the 24 h maximum mixed layer depth are shown for reference. (See text for details.)

- Determine positive DIN increment needed to match layer above, subject to the constraint that total increment decreases with depth.
- Determine increments for phytoplankton, zooplankton and detritus using the DIN-driven local balancing model.

To illustrate the procedure, two example analyses are shown in Figure 3. In Figure 3a a positive surface phytoplankton increment is balanced by negative increments to zooplankton and detritus. No negative increment to DIN is possible beacuse DIN is already depleted. Below the current mixed layer some DIN is available but concentrations are low and the sizes of the negative DIN increments are restricted, despite a relatively large pre-adjustment DIN balancing factor. The analysis preserves the shape of the phytoplankton profile below the current mixed layer, down to the level immediately above the pre-existing deep phytoplankton maximum. At the level of the phytoplankton maximum, the size of the increment is constrained to that at the level above. The other tracer increments differ from those at the level above because the impact of the DIN restriction is reduced as a consequence of the higher DIN concentration.

In the example in Figure 3b, a negative surface increment to phytoplankton is balanced by positive increments to the other tracers in ratios given by the pre-adjustment balancing factors. DIN concentrations are sufficiently high that the DIN restriction has no effect. Below the current mixed layer, the primary increments to DIN are insufficient to bring its concentration up to that at the surface, so secondary increments are required; the positive DIN increments are balanced by negative increments to phytoplankton, zooplankton and detritus. Below the 24 h mixed layer depth maximum, the existence of a sub-surface DIN minimum prior to the analysis constrains the size of the DIN increment to that of the total DIN increment at the level above. However, because primary increments are zero at this depth, the secondary increment is larger than the secondary increment above. Phytoplankton and zooplankton concentrations are too low to supply all of the nitrogen demanded by the pre-adjustment balancing factors (given maximum reduction factors for phytoplankton and zooplankton of 10 and 2 respectively), so a larger fraction of the required nitrogen is taken from detritus at this level.

3. Assimilation experiments

a. Test-bed

An initial off-line evaluation of the material balancing scheme has been carried out in a 1-D test-bed. The test-bed comprises a biogeochemical model forced by physical fields from a 3-D general circulation model. Forcing data representative of 2 different locations along the 20W meridian (30N, 50N) are used. The model is a version of the biogeochemical component of the Hadley Centre Ocean Carbon Cycle Model (HadOCC; Palmer and Totterdell, 2001). It is an NPZD model carrying dissolved inorganic carbon (DIC) and alkalinity as additional tracers coupled to the nitrogen dynamics for determination of the sea surface pCO_2. The carbon:nitrogen (C:N) ratio for each organic compartment is fixed. The version of the model used here differs from that described by Palmer and Totterdell (2001) in having a variable phytoplankton carbon:chlorophyll ratio, reflecting acclimation of the photosynthetic apparatus to the available light and DIN according to the model of Geider *et al.* (1997). In addition, it incorporates the light penetration and photosynthesis model of Anderson (1993), some modifications to the pathways of material resulting from grazing and mortality (Totterdell, *pers. comm.*) and a slow relaxation of DIN towards climatological nitrate (Conkright *et al.*, 1994). Relaxation simulates the effect of unmodeled horizontal DIN fluxes and only occurs below both the 1% light level and the bottom of the upper mixed layer. Model equations are given in Appendix B.

The physical forcing fields are from a 1° global integration of the Forecasting Ocean Assimilation Model system (FOAM; Bell *et al.*, 2000) assimilating temperature data in the form of satellite sea-surface temperature and *in situ* vertical profiles. The biogeochemistry is forced by daily mean solar irradiance, mixed layer depth, surface temperature and surface salinity. The temperature and salinity affect only the derivation of pCO_2 from DIC and

alkalinity and the air-sea flux of CO_2. Although the diel mixed layer depth cycle from the 3-D model is removed by the daily averaging, some variation over the 24 h assimilation time step remains as the daily means are treated as point-in-time values and interpolated linearly. The 1-D test-bed is configured with the same depth levels (see Appendix B) and the same model time-step (1 h) as the 3-D model. After each time step, the tracer values are homogenized within the mixed layer. Partial mixing of the layer below the deepest fully mixed layer introduces some diffusion between the mixed layer and the interior but there is no explicit vertical diffusion scheme. Vertical advection is also omitted.

HadOCC biogeochemistry is included in the 3-D model and the annual cycles obtained in the test-bed are generally similar to those in the 3-D model. However, neither have been properly validated against biogeochemical observations at this stage. The environment for the test-bed experiments should therefore be considered only broadly representative of actual locations in the eastern North Atlantic, with the 30N configuration representing oligotrophic conditions in the sub-tropical gyre and the 50N configuration representing eutrophic conditions at temperate latitudes.

b. Twin experiment design

The tests are based on identical twin experiments in which synthetic data, from a randomly perturbed version of the model run, are assimilated. Twin experiments allow all aspects of an assimilation system's performance to be quantified with reference to known truths. In experiments with real-world data, this is not possible and interpretation is made more complicated by the presence of errors in the physical model. The effect of these errors can seriously compromise assessments of biogeochemical schemes, with respect to their long-term value in the context of improved physical simulations. Twin experiments provide an analytical tool for examining the strengths and weaknesses of individual parts of an assimilation system in isolation, avoiding the need to address all problems simultaneously. Their main disadvantage is their reliance on assumptions about the likely errors in the model. Here, it is assumed that much of the error is associated with the absence of temporal variability in model parameters but there are other numerous other ways that uncertainty could be introduced.

Trajectories representing the true system state evolution were generated by randomly perturbing 10 model parameters during the integration (see Appendix B for details). To allow error statistics for assimilating and non-assimilating runs to be estimated, an ensemble of 100 possible truths was generated in this way. Each parameter was initialized from a normal distribution with a mean $\bar{p}$ equal to the nominal parameter value (i.e. that used in the standard run) and a standard deviation σ_p of 25% of its nominal value. At the start of each day of integration, each parameter value p was both randomly perturbed and weakly relaxed toward its nominal value $\bar{p}$ to get a new value

$$p' = p + 0.5Z\sigma_p - 0.1(p - \bar{p}), \tag{16}$$

where Z is a normally distributed random variable with zero mean and unit standard deviation. The value p' was then adjusted if necessary to bring it within the range $\bar{p} \pm 2\sigma_p$. The same parameter values were used at all depths.

In all assimilation experiments, increments were made to the DIC and alkalinity tracers during the analysis to balance the increments from the nitrogen balancing scheme. For each of the organic tracers (phytoplankton, zooplankton and detritus) a nitrogen increment implies an associated change in carbon, given by the model's fixed C:N ratio for that component. Increments to DIC are applied such that total carbon is conserved at each grid point, given these implicit carbon increments. Alkalinity is incremented in the opposite sense to DIN, consistent with the model dynamics. Assimilation thus affects DIC and alkalinity directly as well as having a post-analysis effect via the impact of the nitrogen increments on the dynamics.

Assimilation results are presented in Section 4 for two complete calendar years. The ensemble runs and the standard run, into which data from the ensemble are to be assimilated, are all started with initial conditions extracted from 3-D model output at the beginning of February in year 1 and allowed to run for 11 months prior to assimilation. The same physical forcing is used for each of the 3 calendar years. Figures 4 and 5 show the true system trajectories for 3 ensemble members for the two calendar years of the assimilation experiments (years 2 and 3).

The data assimilated are daily mean surface concentrations from the truth ensemble with no observation error added. The surface values for the assimilated variables are fully corrected in the analysis so analysis errors in the mixed layer are non-zero for unassimilated variables only. Investigation into the sensitivity of the scheme's performance to missing data and realistic observation errors is beyond the scope of the present paper. In the first experiment, chlorophyll data only are assimilated and chlorophyll increments are converted to phytoplankton increments using the nitrogen:chlorophyll ratio from the model, which is directly proportional to its carbon:chlorophyll ratio. In later experiments, both chlorophyll and phytoplankton nitrogen are assimilated in order to focus on the performance of the balancing scheme itself. The external parameter values used for the nitrogen balancing scheme are given in Table 1. Further parameter values are specified in Appendix A for the probability model used in the pre-adjustment DIN balancing factor determination.

4. Results

a. Overall performance of the chlorophyll assimilation scheme

Figures 6–7 show the performance of the scheme for synthetic daily chlorophyll observations (Experiment A) compared with its performance when both chlorophyll and phytoplankton nitrogen are assimilated (Experiment B). Statistics for the free run (i.e. the standard run with no assimilation) are also shown for reference. The first year of the assimilation (year 2) is preceeded by 11 months with no assimilation and the second is preceeded by 12 months of assimilation. There are only minor differences in the results between years.

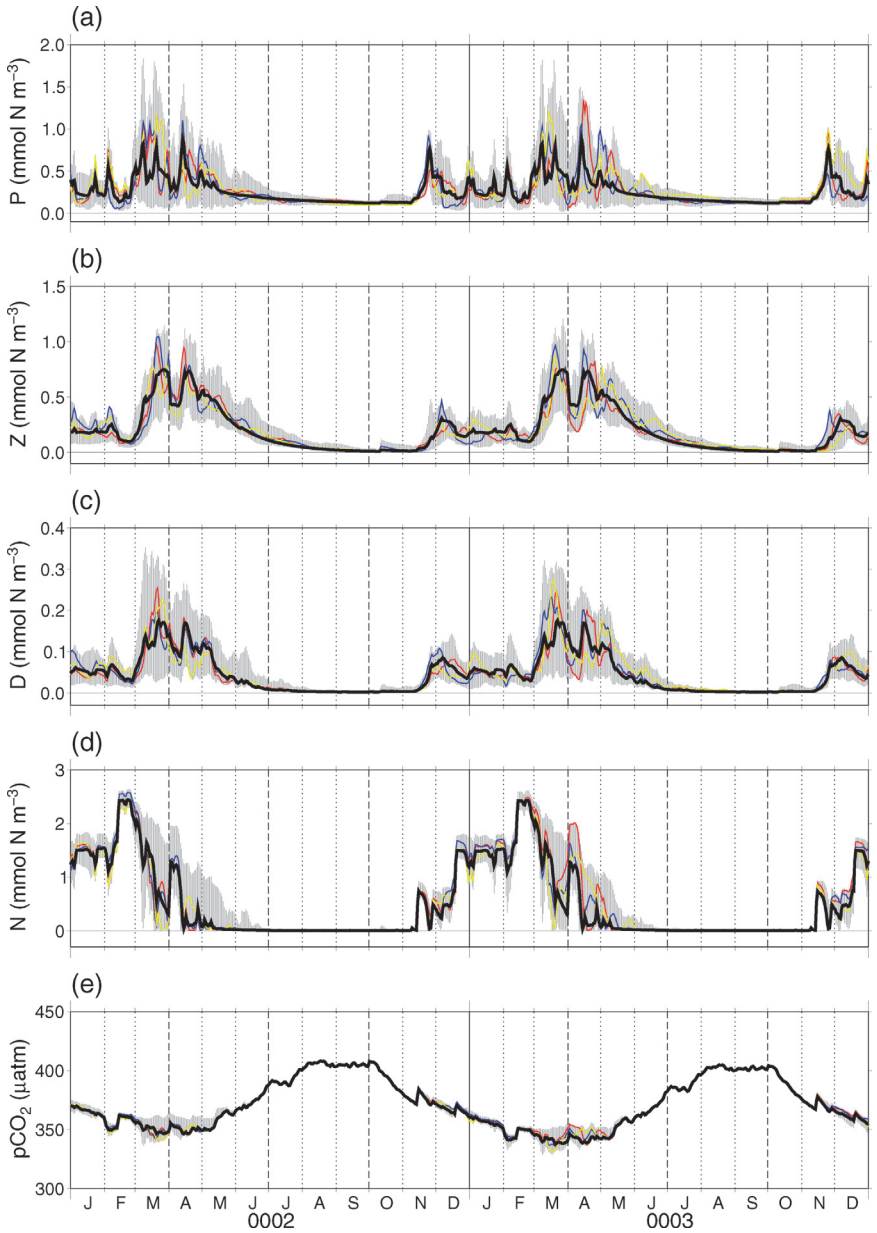

Figure 4. Surface values of (a) phytoplankton, (b) zooplankton, (c) detritus (d) DIN and (e) pCO_2 at 30N 20W for the free run (black) and for 3 randomly selected members of the truth ensemble (colored). The range for the whole 100 member ensemble is shaded in grey.

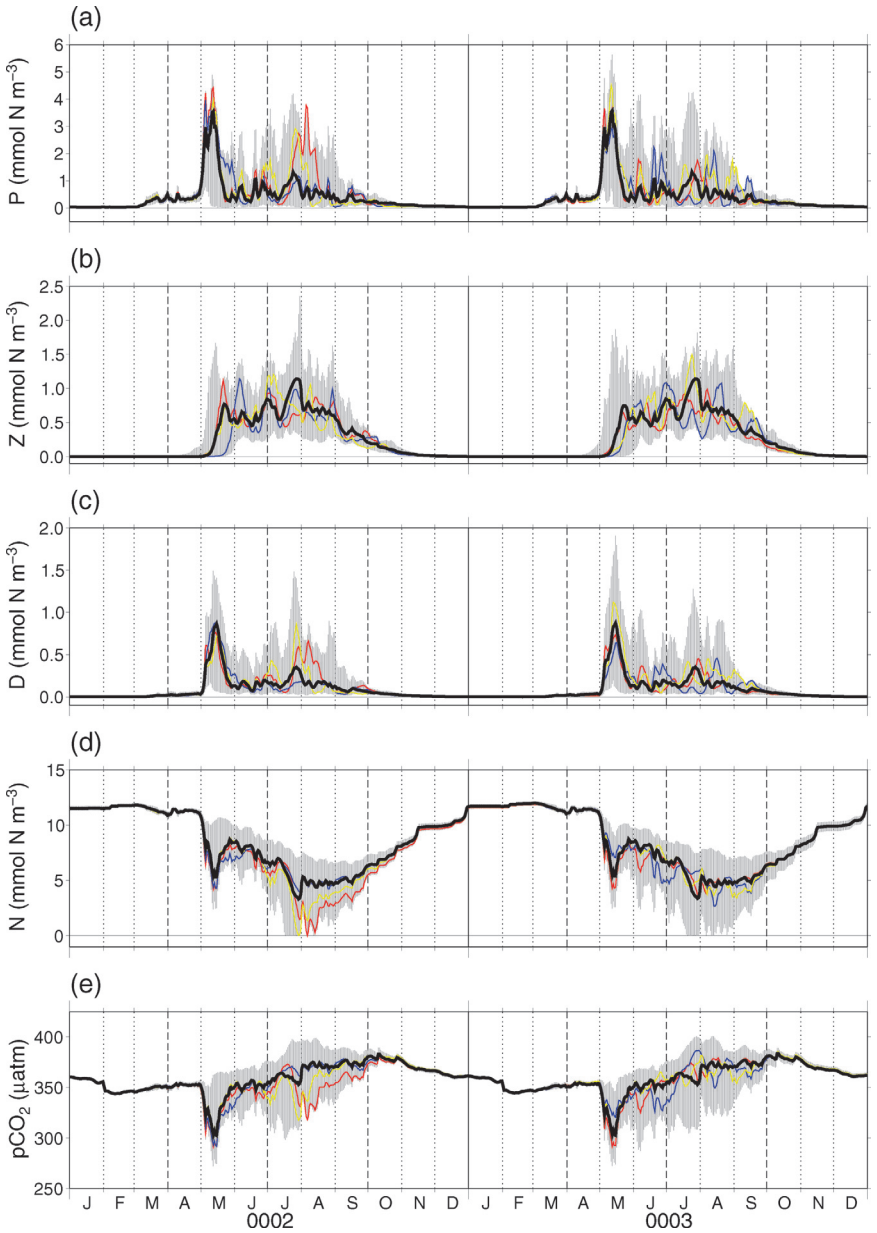

Figure 5. Surface values of (a) phytoplankton, (b) zooplankton, (c) detritus, (d) DIN and (e) pCO_2 at 50N 20W for the free run (black) and for 3 randomly selected members of the truth ensemble (colored). The range for the whole 100 member ensemble is shaded in grey.

Table 1. Nitrogen balancing scheme parameters.

Parameter	Symbol	Value
DIN error fraction	B_{MIN}	0.1
Zooplankton error fraction	f_{Z}	0.7
Nutrient limitation max. reduction factor	R_{Q}	1.1
Nutrient limitation max. amplification factor	A_{Q}	1.1
Zooplankton max. reduction factor	R_{Z}	2
Zooplankton max. amplification factor	A_{Z}	2
Phytoplankton max. reduction factor*	R_{P}	10

*Only applies to secondary increments.

A strong correlation exists between DIN and pCO_2 errors because of coupling between biologically driven changes in DIN and DIC that are imposed by the fixed carbon:nitrogen ratios of the organic compartments. The ratio of these changes varies by only a small amount, the variation being due to different model carbon:nitrogen ratios for phytoplankton, zooplankton and detritus (6.625, 5.625 and 7.5 respectively). The correlation breaks down at low DIN concentrations as uptake of CO_2 by phytoplankton continues to draw down DIC, which is still plentiful, but DIN concentration is determined by a balance between uptake and positive fluxes, only some of which are biological. Positive fluxes can often be dominated by a strong entrainment flux driven by mixed layer depth variations acting on large DIN gradients.

The r.m.s. errors for Experiment A at 50N (Fig. 7) show major improvements in all variables except zooplankton, with no sign of any detrimental effect. For zooplankton, the r.m.s. errors are better than the free run in year 2 but worse in year 3. The situation is less satisfactory at 30N. Here, pCO_2 errors are greatly improved during winter and spring, when DIN concentrations are relatively high, but summer and early autumn r.m.s. errors in pCO_2 are greater than those for the free run. The pattern is reflected in the DIN errors, especially over the summer period and there are adverse effects of assimilation on phytoplankton and zooplankton concentrations in summer too. The DIN error is largely due to a positive bias that starts to develop over winter and reaches a peak in late spring. This is accompanied by a negative bias in zooplankton, indicating too much transfer of nitrogen back to DIN in the case of negative phytoplankton increments or too much transfer of nitrogen from zooplankton to satisfy positive phytoplankton increments. There is a small positive bias in chlorophyll (indicative of a larger bias in the background chlorophyll concentration since the analysis error is zero), showing that negative phytoplankton increments tend to dominate. There is actually less positive bias in phytoplankton than in chlorophyll and sometimes the bias is reversed implying that the negative phytoplankton increments are not always improving the model state. Certainly, there is much less improvement in phytoplankton than at 50N. Although the low latitude summer pCO_2 results are poor compared with the free run, this is a period when the uncertainty associated with biological activity is low (Fig. 4) and the pCO_2 errors are relatively small.

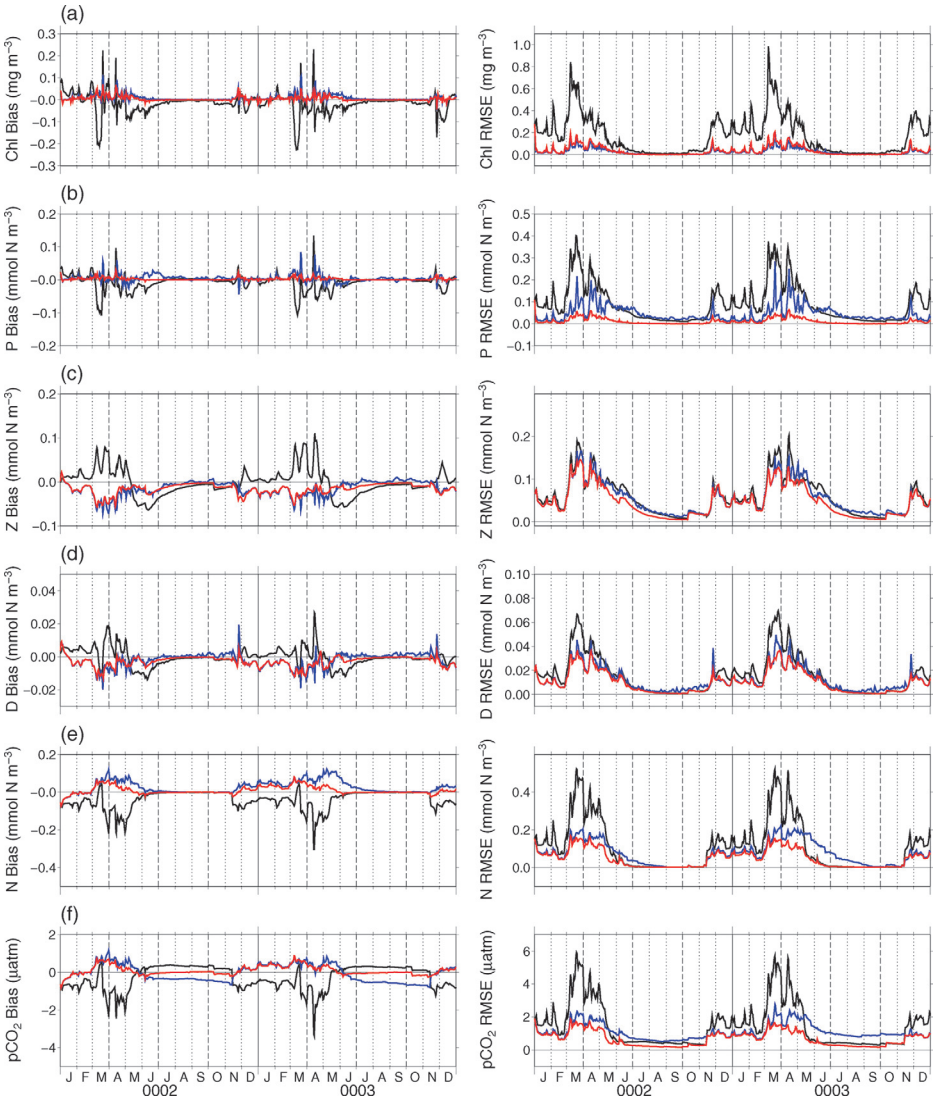

Figure 6. Ensemble bias and r.m.s. errors at 30N 20W for Experiment A: assimilating chlorophyll only (blue) and Experiment B: assimilating chlorophyll and phytoplankton (red). The free run is shown in black. Statistics are shown for daily mean surface values of (a) chlorophyll, (b) phytoplankton, (c) zooplankton, (d) detritus, (e) DIN and (f) pCO_2.

In Experiment B, model errors in the carbon:chlorophyll ratio (or equivalently nitrogen:chlorophyll) do not affect the analysis and assimilation improves pCO_2, DIN and detritus throughout the year at both stations. Zooplankton is also noticeably improved at 30N, though not at 50N. From these results it is clear that, in the twin experiment at least, model

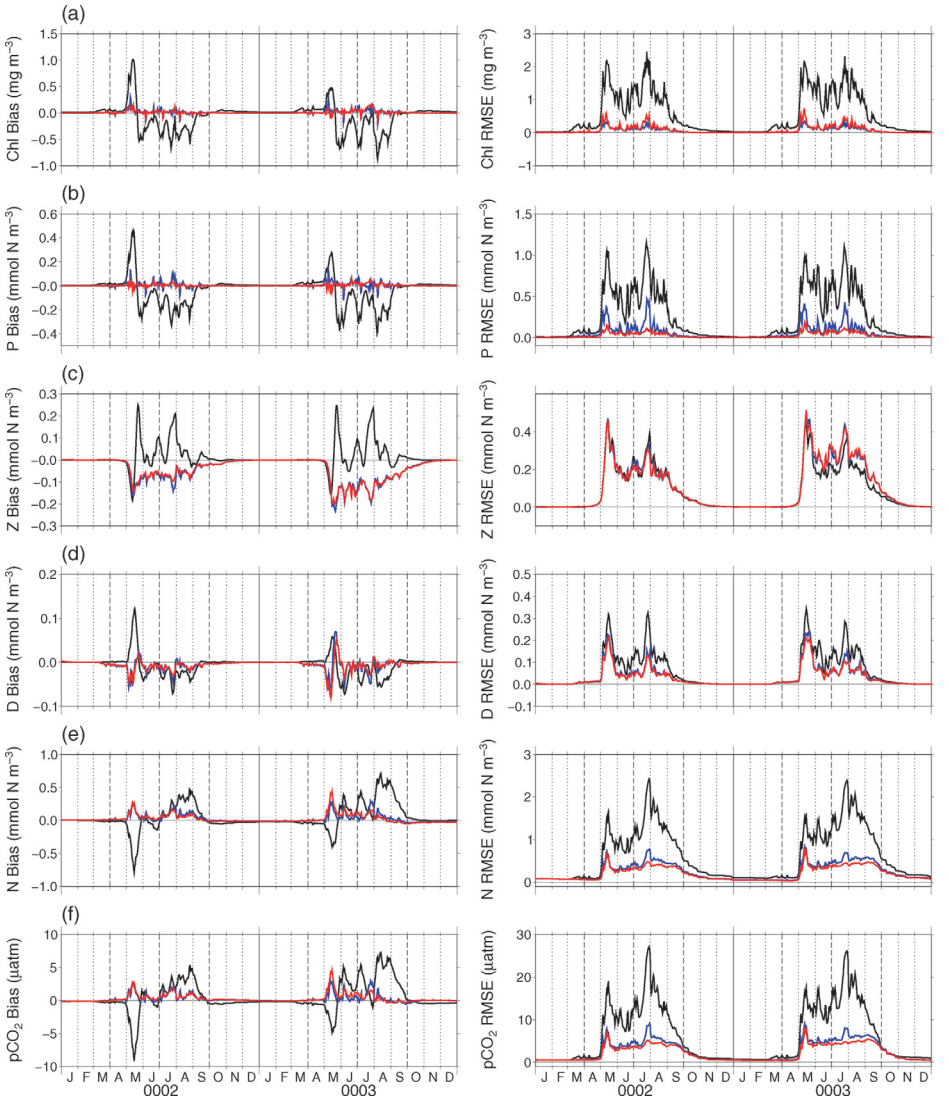

Figure 7. Ensemble bias and r.m.s. errors at 50N 20W for Experiment A: assimilating chlorophyll only (blue) and Experiment B: assimilating chlorophyll and phytoplankton (red). The free run is shown in black. Statistics are shown for daily mean surface values of (a) chlorophyll, (b) phytoplankton, (c) zooplankton, (d) detritus, (e) DIN and (f) pCO_2.

drift in carbon:chlorophyll is a major source of error. The greater variation in this ratio at 30N is the main reason for the difference between the Experiment A results at high and low latitudes. Nutrient limitation of phytoplankton growth at 30N strongly affects the carbon:chlorophyll ratio, increasing its variance and that of the nitrogen:chlorophyll ratio

dramatically. The standard deviation in nitrogen:chlorophyll over the ensemble at 30N is 0.68 mmol N (mg Chl)$^{-1}$, with values ranging from 0.28 to 2.51, compared with a standard deviation of 0.10 mmol N (mg Chl)$^{-1}$ at 50N, with values from 0.26 to just 1.62. The encouraging results for Experiment B show that the scheme has the potential to make major improvements in surface pCO_2 estimates over a wide range of oceanic conditions if an effective method can be found for correcting errors in the carbon:chlorophyll ratio.

b. Impact of the nitrogen balancing scheme

To examine the impact of the nitrogen balancing scheme, the combined chlorophyll and phytoplankton assimilation was repeated with nitrogen balancing switched off (Experiment C). In this experiment, only the phytoplankton and DIC tracers are updated in the analysis; carbon is conserved but nitrogen is not. The results are shown in Figures 8 and 9.

The most obvious point to note is that without nitrogen balancing the DIN errors are much worse than the free run at both stations. These errors are associated with positive biases in the DIN concentration. Moreover, unlike the other experiments where there are only relatively minor differences between the first and second years of assimilation, there are much higher errors in DIN at the beginning of the second calendar year of assimilation at both latitudes. The system does not recover over the winter from the errors introduced by assimilation in the previous year. The positive bias in DIN is attributable to a tendency in the experimental set-up for the free-running model to underestimate phytoplankton. In this situation, the net effect of assimilation without nitrogen balancing is to create excess nitrogen as phytoplankton which is recycled, mostly via zooplankton and/or detritus, to accumulate in the DIN pool.

Importantly for air-sea CO_2 flux estimation, there are marked periods of negative bias in pCO_2 at 30N. These seem to be caused by excess production fueled by excess DIN in spring. There is a less dramatic effect at 50N, where significant nutrient limitation of primary production occurs only late in the summer: positive DIN biases cause negative pCO_2 biases to develop here in late July. It can be seen from these results that, although much of the improvement in pCO_2 is due to improvements in phytoplankton, especially at 50N, the nitrogen balancing scheme is clearly having a beneficial effect. Nitrogen balancing is particularly important for obtaining good estimates of DIN concentration and this has important consequences for pCO_2 in oligotrophic areas.

The other advantage of nitrogen balancing is local nitrogen conservation. Incidences of non-conservation do occur during analyses but are uncommon, particularly when both chlorophyll and phytoplankton biomass are assimilated. This is illustrated by a review of total surface nitrogen increments. In Experiment B, there are no incidences at 50N. At 30N, the maximum total nitrogen increment is 0.016 mmol m^{-3}. The mean increment here over all ensemble members for the 2 year period is tiny (5×10^{-6} mmol m^{-3}). Total nitrogen increments greater than 0.001 mmol m^{-3} are restricted to 0.1% of analyses. In Experiment A, non-conservation is more of an issue with maximum total nitrogen increments of

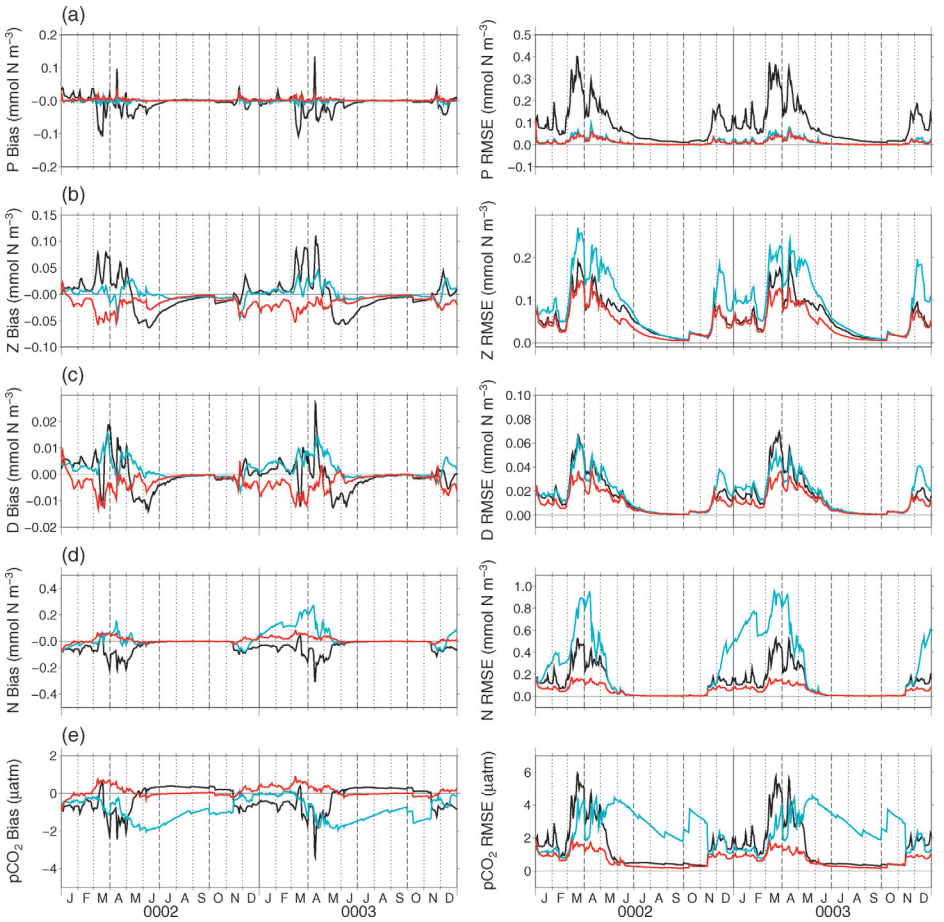

Figure 8. Ensemble bias and r.m.s. errors at 30N 20W for Experiment C: assimilating chlorophyll and phytoplankton without nitrogen balancing (cyan). Results for the same assimilation with nitrogen balancing (Experiment B) are reproduced here for comparison (red). The free run is shown in black. Statistics are shown for daily mean surface values of (a) phytoplankton, (b) zooplankton, (c) detritus, (d) DIN and (e) pCO_2.

1.28 mmol m^{-3} at 30N and as much as 2.78 mmol m^{-3} at 50N. The corresponding means are 0.00042 mmol m^{-3} and 0.00017 mmol m^{-3}. Incidences of total nitrogen increments greater than 0.001 mmol m^{-3} affect 2.3% of analyses at 30N but only 0.02% at 50N.

Any increase in the model's total nitrogen as a result of the non-conservative analyses is ultimately compensated for by the DIN relaxation to climatology, avoiding a detrimental effect on the nitrogen budget. For application in models designed to conserve total nitrogen explicitly, some form of correction would be required for any deficit arising. If it is assumed that the deficit is primarily the result of excessive export from the upper layers due to sinking

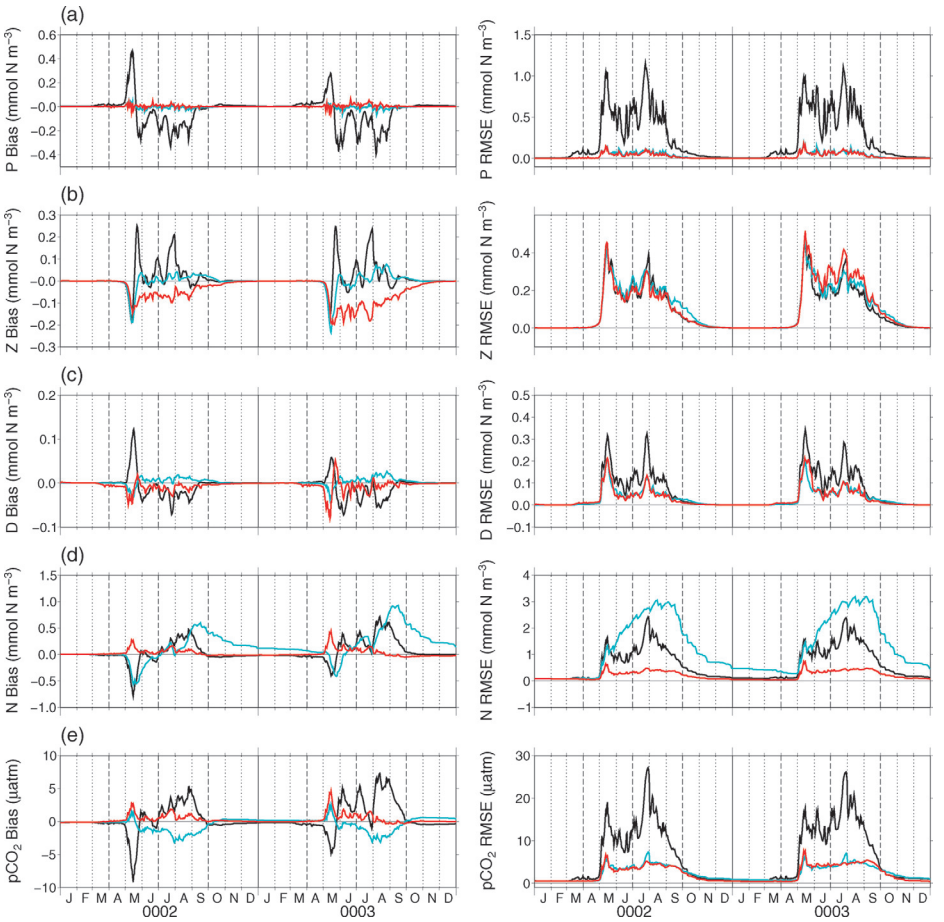

Figure 9. Ensemble bias and r.m.s. errors at 50N 20W for Experiment C: assimilating chlorophyll and phytoplankton without nitrogen balancing (cyan). Results for the same assimilation with nitrogen balancing (Experiment B) are reproduced here for comparison (red). The free run is shown in black. Statistics are shown for daily mean surface values of (a) phytoplankton, (b) zooplankton, (c) detritus, (d) DIN and (e) pCO_2.

particles, this could sensibly take the form of a small adjustment distributed over the whole water column, maintaining relative tracer concentrations.

c. Balancing factor adjustment

Although nitrogen balancing appears to have a beneficial effect, the individual contributions of the pre-adjustment balancing factor determination and balancing factor adjustment phases are less clear. These have been examined in some detail with reference to Experiment B. The extent of balancing factor adjustment occurring in Experiment B is examined

Table 2. DIN balancing factor adjustments in Experiment B (surface analyses only).

	30N		50N		
	Small ΔP 10^{-4} to 0.1 mmol N m^{-3}	Medium ΔP 0.1 to 0.5 mmol N m^{-3}	Small ΔP 10^{-4} to 0.1 mmol N m^{-3}	Medium ΔP 0.1 to 0.5 mmol N m^{-3}	Large ΔP > 0.5 mmol N m^{-3}
Number of analyses	69429	2403	58893	9501	233
Fraction adjusted	33%	31%	5%	1%	1%
Number of -ve adjustments	22585	734	47	109	2
Mean -ve adjustment	−0.23	−0.32	−0.32	−0.32	−0.49
Largest -ve adjustment	−0.86	−0.90	−0.84	−0.87	−0.53
Number of +ve adjustments	22	0	2637	17	0
Mean +ve adjustment	0.14	–	0.30	0.01	–
Largest +ve adjustment	0.36	–	0.60	0.05	–

first and the effect of the pre-adjustment balancing factors is then considered in the following section. Adjustment statistics for the DIN balancing factor b_N are shown in Table 2. Table 3 shows the same statistics for adjustment of the zooplankton increment as a fraction of the total increment to zooplankton and detritus. This fraction, referred to as the fractional zooplankton increment, is given by

$$f'_Z = \frac{b_Z}{b_Z + b_D}. \tag{17}$$

It's pre-adjustment value is the prescribed zooplankton error fraction $f_Z(=0.7)$. Because the size of the phytoplankton increment determines the sensitivity of the other tracer increments to their respective balancing factors, any given adjustment will have a greater influence on the model state when phytoplankton increments are large. To aid appreciation of their significance or otherwise, the adjustment statistics are therefore tabulated according to different ranges of the phytoplankton increment. The statistics are for all 100 ensemble members and both years of the assimilation. Only surface layer analyses are included.

The first thing to note is that adjustment occurs only in the minority of analyses. Nevertheless, when it does occur the adjustments can be large. Negative adjustments to b_N occur as a result of restrictions to the change in the model phytoplankton's DIN limitation factor, whereas positive adjustments occur in response to negative adjustments in the zooplankton and/or detritus balancing factors in the case where both zooplankton and detritus increments are restricted. Negative adjustments dominate at 30N where significant DIN limitation is

Table 3. Adjustments to the fractional zooplankton increment f'_Z in Experiment B (surface analyses only).

	Small ΔP 10^{-4} to 0.1 mmol N m^{-3}	Medium ΔP 0.1 to 0.5 mmol N m^{-3}	Small ΔP 10^{-4} to 0.1 mmol N m^{-3}	Medium ΔP 0.1 to 0.5 mmol N m^{-3}	Large ΔP > 0.5 mmol N m^{-3}
Number of analyses	69429	2403	58893	9501	233
Fraction adjusted	1%	1%	26%	28%	80%
Number of -ve adjustments	580	19	15113	2640	187
Mean -ve adjustment	−0.42	−0.33	−0.62	−0.66	−0.66
Largest -ve adjustment	−0.70	−0.70	−0.70	−0.70	−0.70
Number of +ve adjustments	34	2	0	0	0
Mean +ve adjustment	0.09	0.08	–	–	–
Largest +ve adjustment	0.18	0.09	–	–	–

common and, as expected, they are rare at 50N where more eutrophic conditions prevail. Positive adjustments are much more common at the northerly station.

Negative adjustments to f'_Z occur as a result of the impact of zooplankton restrictions on b_Z; positive adjustments occur in response to negative b_D adjustments. Clearly negative adjustments to f'_Z are much more common and at 50N there are no positive adjustments. At either station, the negative adjustments can be large enough to remove virtually all of the zooplankton increment implied by the pre-adjustment balancing factor. However, the result does not imply that the f_Z parameter is generally too high, as the incidence of adjustment is actually rather low. At 30N, adjustment of f'_Z is particularly rare (1% of analyses). At 50N, f'_Z is adjusted in a higher proportion of analyses, especially when the phytoplankton increment is large.

The higher frequency of negative adjustments to f'_Z at 50N can be explained with reference to the model runs shown in Figure 5. The annual zooplankton cycle here is characterized by extremely low winter-time concentrations that remain much smaller than those of phytoplankton for a long period in early spring. The same tendency is true in the assimilation runs, making frequent negative adjustment of b_Z inevitable because the analysis is not permitted to change the zooplankton concentration by more than a factor of two. f'_Z is reduced as a consequence except in cases when there is a similar or greater relative adjustment to b_D because of insufficient detritus. The imposed zooplankton restriction plays an important role because of the scheme's reliance on a constant f_Z. However, the parameter values controlling the restriction (R_Z and A_Z) are essentially arbitrary so the scheme's dependence

Table 4. Sensitivity of surface pCO_2 error statistics to pre-adjustment balancing factor parameterization.

	30N		50N	
	Bias	R.m.s. error	Bias	R.m.s. error
Parameterization	μ atm	μ atm	μ atm	μ atm
Control (Expt. B)	0.08	0.82	0.31	2.87
No balancing (Expt. C)	−0.91	2.74	−0.38	2.95
$f_Z = 0$	0.24	1.03	0.36	3.95
$f_Z = 1$	0.07	0.84	0.03	2.94
Turnover term omitted	0.03	0.80	−0.08	3.42
Pre-adj. $b_N = 0.1$	−0.26	1.04	−2.37	8.98
Pre-adj. $b_N = 1$	−0.07	1.24	−0.36	3.25
Pre-adj. $b_N = 0.6$	−0.21	0.89	−0.93	3.61
Pre-adj. $b_N = 0.8$	−0.19	0.94	−0.17	2.90

on them is undesirable. Its behaviour suggests that it might benefit from a more sophisticated zooplankton error fraction parameterization.

The lack of freedom to adjust zooplankton due to its low concentration explains the relatively high incidence of positive b_N adjustments at 50N. However, the incidence is low compared with the number of negative adjustments to f'_Z. In most cases, the detritus factor compensates for reduction in b_Z either because the zooplankton and detritus increments are positive or because the detritus concentration is sufficiently high not to introduce a detritus restriction. The number of positive b_N adjustments indicates the total number of analyses in which a zooplankton restriction affects the DIN concentration, while the number of negative f'_Z adjustments indicates the minimum number of analyses in which the zooplankton increment is restricted. From the numbers in Tables 2 and 3, it can therefore be inferred that the zooplankton restriction affects the DIN concentration in at most 14% of cases.

d. Sensitivity to pre-adjustment balancing factors

To examine the influence of the pre-adjustment balancing factor parameterization on the results, a number of sensitivity experiments were performed with Experiment B as a control. In Experiment B, the zooplankton error fraction parameter f_Z was 0.7. This value gave the minimum pCO_2 r.m.s. error values at both stations independently. pCO_2 error statistics for experiments in which f_Z was set to its minimum and maximum values, 0 and 1, are presented in Table 4. The table also summarizes the effect of using simpler parameterizations for b_N. Again, the statistics are for all 100 ensemble members and both assimilation years. The statistics for the control experiment and Experiment C, in which there is no nitrogen balancing, are shown for comparison.

The upper value of f_Z ($f_Z = 1$) causes only a small increase in pCO_2 error over the control experiment (about 2% at 30N and less than 1% at 50N) and actually reduces the overall

positive bias, especially at the more northerly station. However, the apparent improvement here is not due to any reduction in the positive peaks in bias occurring in May (Experiment B in Figs. 7f and 9f) but to the development of a compensating negative bias in late summer (data not shown). This occurs in both years of the assimilation but is greater in the second year, reaching -2 μatm and remaining below -1 μatm for a period of about 40 days. Using the lower value of f_Z ($f_Z = 0$) causes much larger increases in the pCO_2 error (26% at 30N and 38% at 50N). There is an adverse impact on the positive bias too, especially in the south where it is larger by a factor of 3.

Two alternatives to the standard parameterization of the pre-adjustment DIN balancing factor were examined. In the first, the turnover term in the DIN balancing function (Eq. 20) is omitted which restricts the upper bound of the balancing factor to 1. In the second, the pre-adjustment DIN balancing factor was kept constant but treated as a tunable parameter. Different b_N values were required to give the minimum pCO_2 r.m.s. error values for the different stations. The optimal pre-adjustment factor at 30N was 0.6, while a factor of 0.8 gave the lowest error at 50N. The results for these values are tabulated along with those for the minimum value ($b_N = 0.1$) and the maximum value possible with zero turnover offset ($b_N = 1$).

Omitting the turnover term from the DIN balancing function actually seems to have a beneficial effect at 30N where it reduces the pCO_2 r.m.s. error by about 2.5%. However, this is outweighed by a 19% increase at 50N, where omitting nitrogen balancing altogether only increases the error by about 3.5%. Interestingly though, improvements in bias over the control are seen at both stations. The apparent improvements at 50N are a consequence of a similar temporal pattern of positive and negative bias as that described above for $f_Z = 1$ but the reduced bias at 30N is temporally more consistent, suggesting that the positive bias here is the result of over-correction for the turnover effect.

The minimum r.m.s. error in pCO_2 obtainable with a constant pre-adjustment balancing factor is greater than that for the standard parameterization used in the control experiment by about 8.5% at 30N and 2.5% at 50N. Relatively large negative biases are also incurred at both stations. Using extreme values increases the errors further, with a value of 0.1 giving very poor performance at 50N. For this low value, again there are large negative biases at both stations. Much smaller biases are seen for $b_N = 1$, similar in magnitude to those for the control but of opposite sign.

In general, the inferior performance of the constant pre-adjustment DIN balancing factor parameterization demonstrates the value of the calculations in the first phase of balancing factor determination. In combination with the adjustment statistics presented in the previous section, these results show that both phases play an important role.

5. Discussion

A computationally inexpensive nitrogen balancing scheme for ocean color data assimilation has been developed. Updating a model's nitrogen variables on the basis of information

relating to phytoplankton only is challenging. Much of the model error affecting DIN, zooplankton and detritus does not affect phytoplankton directly and some of the errors that do will cancel out leaving no evidence in the phytoplankton concentration. Even in the idealized case of a perfect phytoplankton analysis with optimal balancing factors, some analysis error will therefore remain in the other variables. These errors can accumulate over time, with the consequence that increments correcting for recent errors can sometimes increase the overall error. Essentially, observations of phytoplankton properties only cannot fully constrain an imperfect model.

Despite these inherent problems, the tests show that the nitrogen balancing scheme performs well in the sense that, on average, it improves estimates for most of the biogeochemical variables under most conditions in a way that cannot be achieved in the twin experiments by a simple scheme without nitrogen balancing. This demonstrates that the improved performance is not solely attributable to the improvements in phytoplankton. The results suggest that univariate assimilation schemes could introduce much larger biases in surface pCO_2 with serious implications for air-sea flux estimates. Nitrogen balancing is clearly beneficial and the scheme's performance might be further improved by optimizing its external parameters. Although the scheme is designed to conserve nitrogen at individual grid points, it has performed well in the presence of errors in total nitrogen caused by errors in detritus concentration and detrital sinking rates. In real-world applications, errors in total nitrogen will also occur as a consequence of errors in the physical simulation.

The scheme described here is a baseline scheme. Non-zero analysis error in phytoplankton has not been explicitly allowed for in the calculation of the pre-adjustment balancing factors. This is partly because of an expectation that it is often likely to be small relative to the model error introduced during the assimilation time-step and partly because of the difficulty in estimating its variance in advance of the scheme's implementation in a 3-D assimilation system. In the experiments presented here where both chlorophyll and phytoplankton nitrogen are assimilated, the analysis error is forced to be zero. Significant analysis error in phytoplankton is present in the chlorophyll only assimilation experiment though and it will certainly be present in real-world applications. Ignoring this source of error may mean that the analysis gives excessive weight to the recent model dynamics and to current observations. One relatively simple solution might be to carry forward pre-adjustment balancing factors from the previous analysis and combine them with the new factors with appropriate weightings.

It is useful to compare the approach used here with the more traditional Kalman filter algorithm employed by Natvik and Evensen (2003). The Kalman filter uses a purely statistical approach to solving the problem of updating the unassimilated variables, while the nitrogen balancing scheme places more emphasis on material conservation and the relationship between the analysis increments and the actual background state. Natvik and Evensen (2003) did take the model state into account though, in that their EnKF analysis was followed by a step in which negative fields were set to zero. The EnKF analysis itself conserves the total inventory of nitrogen (because this will be identical in all ensemble members used to

calculate the covariances) but does not conserve nitrogen at individual grid-points. While the nitrogen balancing scheme is designed primarily to correct for model error occurring since the previous analysis and ignores the issue of analysis error, the EnKF treats the analysis error explicity: the ensemble representing the error covariances is evolved using the model to forecast the background statistics for the next analysis. Model error can be included in the EnKF and other Kalman filter-based schemes but the model error covariances must be prescribed.

The extent to which Kalman filter-based schemes assimilating chlorophyll only will be able to update unassimilated variables reliably in the analysis remains to be seen. Eknes and Evensen (2002) have shown in 1-D twin experiments that the EnKF has the potential to handle the strong non-linearities present in biogeochemical models and is able to track zooplankton and DIN in an NPZ model when only phytoplankton data are assimilated. Other types of Kalman filter too have shown promising results in twin experiments where synthetic ocean color data are assimilated into more complex 3-D models (Carmillet *et al.*, 2001; Hoteit *et al.*, 2005). In real-world applications, the main problem is likely to be the dependency of the results on the assumed characteristics of the model error. Present understanding of the error characteristics of biogeochemical models is limited and may inhibit the development of robust Kalman filter-based schemes. Nevertheless, the strengths of the Kalman filter should not be overlooked and combining Kalman filter techniques for evolving error statistics with the nitrogen balancing scheme might lead to better performance than is possible using either method on its own.

Another state estimation technique which should be considered is four-dimensional variational assimilation (4DVAR). It has been applied with some success to non-linear problems in atmospheric prediction, as discussed by Park and Zupanski (2003), but has yet to be evaluated for biogeochemical models. A 4DVAR analysis involves a weighted minimization of the misfit between the analysis and background states and the misfit of the model forecast for some period after the analysis time to observations within that period. The method is efficient for non-linear problems over short time intervals. It allows dynamical constraints from the model to contribute directly to the determination of the increments, reducing their dependence on the specified background error covariances and the observations available at the analysis time. Weak-constraint 4DVAR techniques can be used to allow for model error but, as with the Kalman filter schemes, the specification of model error statistics is likely to be a difficult issue. A hybrid scheme combining the strengths of the nitrogen balancing scheme with those of 4DVAR is conceivable.

The susceptability of the assimilation to errors in the model nitrogen:chlorophyll ratio is an area of some concern. In the present work, the nitrogen:chlorophyll ratio is proportional to the carbon:chlorophyll ratio and both are controlled by a phytoplankton acclimation model, in which the biomass specific rate of change of chlorophyll depends on the biomass specific growth rate and the ambient light. Improvements in the DIN concentration due to chlorophyll assimilation have some beneficial effect on this ratio via the growth rate. However, a more direct means of correction is desirable. Ocean color products other than chlorophyll

may provide an effective way to address the problem. The most direct solution would be to use ocean color-based estimates of phytoplankton carbon (Behrenfeld *et al.*, 2005) in conjunction with the chlorophyll product. In addition, ocean color information relating to the light field or perhaps even to the biomass specific growth rate of the phytoplankton directly could potentially be used to improve the performance of the acclimation model. Any information regarding the biomass specific growth rate could also be used to improve the nitrogen balancing scheme itself by modifying the probability model for growth and loss error components used in the DIN balancing factor calculation.

In conclusion, assimilation of satellite ocean color data in ocean general circulation models promises great benefits in the context of efforts to monitor and predict carbon fluxes in the global climate system. The most effective methods for combining these and other earth observation data with models are yet to be established but it is clear that sequential and inverse methods will both play an important role. Our initial experiments show the nitrogen balancing scheme to be a valuable sequential assimilation tool. Such tools are best applied to accurate models: model improvement through application of inverse methods should improve the performance of state estimation schemes in general, by reducing bias in the background state. For the nitrogen balancing scheme in particular, more accurate models will also provide better estimates of growth and loss rate for estimating the optimal DIN balancing factor. Improvements to the biogeochemical models will also be particularly important in long-term forecast applications where the sensitivity to initial conditions provided by a sequential assimilation system is low.

Acknowledgments. The authors wish to acknowledge the contribution of the referees in providing very helpful and constructive comments. Thanks are also due to Ian Totterdell for support with the test model and to Matt Martin, Adrian Hines, Jim Gunson, Peter Challenor and Keith Haines for their suggestions and advice on various aspects of the work and its presentation. The work was supported by the UK Natural Environment Research Council via the NERC Centre for Observation of Air-sea Interactions and Fluxes.

APPENDIX A

Determination of the pre-adjustment DIN balancing factor

Three simplifying assumptions are made for the purposes of defining the DIN balancing function $B(x, y)$ and the phytoplankton error component probability distribution $p(x, y)$: (1) relative errors in phytoplankton are small, (2) variations in phytoplankton over the assimilation time-step are small relative to the concentration and (3) recently entrained phytoplankta with significant histories of sub-surface growth and loss rates over the assimilation period make up only a small fraction of the stock. Assumption (1) allows the interaction between X and Y via the concentration to be ignored so they can be treated as independent variables. The other assumptions then allow x to be related directly to the error in the mean

phytoplankton specific growth rate and y to the error in the mean phytoplankton specific loss rate:

$$x = \Delta t P_0 \left(G_0^\bullet - G^\bullet\right) \tag{18}$$

and

$$y = -\Delta t P_0 \left(L_0^\bullet - L^\bullet\right), \tag{19}$$

where $G^\bullet$ and $L^\bullet$ are the unknown true mean specific growth and loss rates for the mixed layer.

The assumptions are largely pragmatic, being introduced in order to avoid complexity that cannot easily be justified given the inherent uncertainties in the process of estimating optimal balancing factors. They are not considered generally robust. The validity of assumption (1) depends on the performance of the assimilating model so we might expect the balancing scheme to perform better as the model is improved. Assumption (2) is reasonable in most circumstances but is violated during intense bloom periods, when phytoplankton concentration may double in a day or less. Assumption (3) is based on the tendency for phytoplankton concentration to be lower below the mixed layer than within it. It is violated during significant entrainment of stock from a deep phytoplankton maximum or by a combination of relatively high sub-surface concentrations with a large relative increase in the depth of mixing over the assimilation time-step.

a. DIN balancing function

$$\begin{aligned} B\left(x, y, P_0, G_0^\bullet, L_0^\bullet\right) = {} & u_G(x, y) + (1 - u_G(x, y)) B_{MIN} \\ & + 0.5 \Delta t (1 - B_{MIN}) T_1^\bullet \left(x, y, P_0, G_0^\bullet, L_0^\bullet\right) \end{aligned} \tag{20}$$

where u_G is the fraction of the phytoplankton error attributed to errors in the growth rate, B_{MIN} is the DIN error fraction (the expected DIN fraction of the phytoplankton loss error), $T_1^\bullet$ is the estimated phytoplankton specific turnover rate and Δt is the assimilation time step. If x and y have the same sign then growth and loss errors are additive and

$$u_G = \frac{x}{x + y}. \tag{21}$$

Otherwise growth and loss errors partly cancel and $u_G = 1$ if $|x| > |y|$ or $u_G = 0$ if $|x| < |y|$. The last term in B is a positive offset designed to correct for the effect of phytoplankton error on the turnover from DIN to zooplankton and detritus (with a fraction B_{MIN} going back to DIN). The mean phytoplankton error for calculating the correction is taken to be half that at the analysis time.

The true phytoplankton specific turnover rate is the balanced fraction of the phytoplankton specific growth rate, *i.e.* min ($G^\bullet$, $L^\bullet$). Instead of the model estimate $T_0^\bullet = \min(G_0^\bullet, L_0^\bullet)$ a refined estimate based on Equations 18 and 19 is used:

$$T_1^\bullet = \min\left(G_0^\bullet - \frac{x}{\Delta t\, P_0}, L_0^\bullet + \frac{y}{\Delta t\, P_0}\right). \tag{22}$$

b. Error component probability model

The joint p.d.f. $p(x, y)$ is the product of p.d.f.s $p(x)$ and $p(y)$ describing the distributions of X and Y respectively (since X and Y are treated as independent). The magnitude of the rate errors is expected to increase as the rates increase, consistent with the model dynamics in which both rates are products of uncertain factors. Log-normal distributions are therefore used.

The p.d.f. for the phytoplankton error component attributed to growth rate error is

$$p(x) = \frac{1}{x_{\mathrm{MAX}} - x} N\left(\frac{\log(x_{\mathrm{MAX}} - x) - \mu_{\mathrm{G}}}{\sigma_{\mathrm{G}}}\right) \tag{23}$$

$$x_{\mathrm{MAX}} = \Delta t\, P_0 G_0^\bullet \tag{24}$$

$$\mu_{\mathrm{G}} = \log\left(\Delta t\, P_0 G_1^\bullet\right) - \frac{\sigma_{\mathrm{G}}^2}{2} \tag{25}$$

where N is the normal distribution with zero mean and unit standard deviation and σ_{G} is an external parameter specifying the uncertainty of the growth rate estimate. x_{MAX} is the maximum value of x from Eq 18, occurring when the true growth rate is zero. $G_1^\bullet$ is a model-based estimate of $G^\bullet$:

$$G_1^\bullet = \beta_{\mathrm{G}} + \frac{G_0^{\bullet 2}}{4\beta_{\mathrm{G}}}, \quad G_0^\bullet < 2\beta_{\mathrm{G}} \tag{26}$$

$$G_1^\bullet = G_0^\bullet, \quad G_0^\bullet >= 2\beta_{\mathrm{G}} \tag{27}$$

where β_{G} is a low growth bias correction parameter. $G_1^\bullet$ diverges from $G_0^\bullet$ to allow for expected bias due to a non-vanishing error variance in a positive quantity. From Eq. 18, the expected value of the true specific growth rate based on the distribution of X is

$$\frac{x_{\mathrm{MAX}} - E(X)}{\Delta t\, P_0}.$$

The definition of μ_{G} (Eq. 25) equates this to $G_1^\bullet$.

Table 5. Probability model parameters.

Parameter	Symbol	Value
Low rate bias correction for growth rate estimator	β_G	0.05 d^{-1}
Low rate bias correction for loss rate estimator	β_L	0.05 d^{-1}
Error s.d. of estimated growth rate	σ_G	0.2 $\log_{10}$ units
Error s.d. of estimated loss rate	σ_L	0.4 $\log_{10}$ units

Similarly, for the error component attributed to loss rate error

$$p(y) = \frac{1}{y - y_{MIN}} N\left(\frac{\log(y - y_{MIN}) - \mu_L}{\sigma_L}\right) \tag{28}$$

$$y_{MIN} = -\Delta t\, P_0 L_0^\bullet \tag{29}$$

$$\mu_L = \log\left(\Delta t\, P_0 L_1^\bullet\right) - \frac{\sigma_L^2}{2} \tag{30}$$

where the external parameter σ_L specifies the uncertainty in the loss rate estimate. y_{MIN} is the minimum value of y from Eq. 19, occurring when the true loss rate is zero. $L_1^\bullet$ is the model based estimate of $L^\bullet$:

$$L_1^\bullet = \beta_L + \frac{L_0^{\bullet 2}}{4\beta_L}, \quad L_0^\bullet < 2\beta_L \tag{31}$$

$$L_1^\bullet = L_0^\bullet, \quad L_0^\bullet >= 2\beta_L \tag{32}$$

where β_L is the low loss bias correction at $L_0^\bullet = 0$. Eq. 30 ensures that the expected value of the true specific loss rate

$$\frac{E(Y) - y_{MIN}}{\Delta t\, P_0}$$

is equated to $L_1^\bullet$.

The parameter values used for the error component probability model in the present study are given in Table 5.

APPENDIX B

HadOCC biogeochemical model

The process parameterizations and time evolution of the biogeochemistry at vertical grid points in the test model (depths: 5, 15, 25, 35, 48, 67, 96, 139, 204, 301, 447 m) are as specified below. Vertical transport fluxes, i.e. sinking and mixing, are omitted for clarity. Table 6 gives the values of the model parameters. The parameterizations are described in more detail by Palmer and Totterdell (2001).

Table 6. Test model parameters.

Parameter	Symbol	Value	Perturbed
C:N ratio for phytoplankton	θ_P	6.625	no
C:N ratio for zooplankton	θ_Z	5.625	no
C:N ratio for detritus	θ_D	7.5	no
Maximum photosynthetic rate	V_{max}	2 d^{-1}	yes
Initial slope of photosynthesis v irradiance curve	α	5.56 mg C (mg Chl)$^{-1}$ (E m^{-2})$^{-1}$	yes
Half-saturation conc. for nutrient uptake	k_N	0.1 mmol N m^{-3}	yes
Conc. dependent phytoplankton specific mortality	m_0	0.05 d^{-1}(mmol N m^{-3})$^{-1}$	yes
Phytoplankton specific respiration	η	0.05 d^{-1}	no
Base zooplankton specific mortality	μ_1	0.05 d^{-1}	yes
Conc. dependent zooplankton specific mortality	μ_2	0.3 d^{-1}(mmol N m^{-3})$^{-1}$	yes
Maximum grazing rate	g_{max}	0.8 d^{-1}	yes
Half-saturation conc. for grazing	k_F	0.5 mmol N m^{-3}	yes
Biomass-equivalent:N ratio for phytoplankton[1]	B_P	1	no
Biomass-equivalent:N ratio for zooplankton[1]	B_Z	0.87	no
Biomass-equivalent:N ratio for detritus[1]	B_D	1.11	no
Fraction of grazed material ingested	ϕ_I	0.77	no
Assimilation efficiency for phytoplankton	β_P	0.9	no
Assimilation efficiency for detritus	β_D	0.65	no
Remineralization rate	$\lambda(z)$	0.1 d^{-1} (z < 100 m); 8.58/z d^{-1} (z > 100 m)	no
Nutrient relaxation rate	$r(z)$	0 (z < MLD or z < 1% lt. level); 0.0167 d^{-1}	no
Carbonate precipitated per unit primary prod.	γ_C	0.013	yes
Detrital sinking velocity		10 m d^{-1}	yes

[1]parameter derived from C:N ratio

Phytoplankton specific growth: $G^\bullet = J(V_{max}, \alpha)Q$, where J is the maximum light-limited photosynthesis, calculated according to Anderson (1993), and Q is the DIN limitation factor;

$$Q = \frac{N}{N + k_N}.$$

Phytoplankton mortality: $M_P = mP^2$; $m = 0$ for $P <= 0.01$ mmol N m^{-3}, otherwise $m = m_0$.

Zooplankton mortality: $M_Z = \mu_1 Z + \mu_2 Z^2$.

Grazing: phytoplankton and detritus losses due to herbivorous zooplankton activity are $H_P = hP$ and $H_D = hD$ repectively, where h is the grazing rate per unit food concentration:

$$h = \frac{B_Z Z}{F_{tot}} g_{max} \frac{F^2}{F^2 + k_F^2};$$

$F = \max(0, F_{tot} - F_{threshold})$, where $F_{tot} = B_P P + B_D D$ and $F_{threshold} = 0.01\,\text{mmol N m}^{-3}$.

Phytoplankton specific loss: $L^\bullet = mP + \eta + h$.

Nitrogen equations:

$$\frac{dP}{dt} = (G^\bullet - L^\bullet)P$$
$$= G^\bullet P - M_P - \eta P - H_P \tag{33}$$
$$\frac{dZ}{dt} = \phi_I(\beta_P H_P + \beta_D H_D) - M_Z \tag{34}$$
$$\frac{dD}{dt} = \frac{\theta_P}{\theta_D}(0.99 M_P) + \frac{\theta_Z}{\theta_D}(0.33 M_Z) + \frac{\theta_P}{\theta_D} a_{PD} H_P + (a_{DD} - 1) H_D - \lambda D \tag{35}$$
$$\frac{dN}{dt} = \left\{0.01 + \left(1 - \frac{\theta_P}{\theta_D}\right) 0.99\right\} M_P + \eta P + \left\{0.67 + \left(1 - \frac{\theta_Z}{\theta_D}\right) 0.33\right\} M_Z$$
$$+ 0.1(1 - \phi_I)(H_P + H_D) + \left(1 - \frac{\theta_P}{\theta_D}\right) a_{PD} H_P$$
$$+ \lambda D - G^\bullet P - r(N - N_{clim}) \tag{36}$$

where $a_{PD} = 0.9(1 - \phi_I) + (1 - \beta_P)\phi_I$ and $a_{DD} = 0.9(1 - \phi_I) + (1 - \beta_D)\phi_I$ and N_{clim} is the climatological nitrate.

Equations for DIC (C) and alkalinity (A):

$$\frac{dC}{dt} = \theta_P(0.01 M_P) + \theta_P \eta P + \theta_Z(0.67 M_Z)$$
$$+ 0.1(1 - \phi_I)(\theta_P H_P + \theta_D H_D) + \phi_I\{(\theta_P - \theta_Z)\beta_P H_P + (\theta_D - \theta_Z)\beta_D H_D\}$$
$$+ \theta_D \lambda D - (1 + \gamma_C)\theta_P G^\bullet P \tag{37}$$
$$\frac{dA}{dt} = -2\gamma_C \theta_P G^\bullet P - \frac{dN}{dt}. \tag{38}$$

REFERENCES

Allen, J. I., M. Eknes and G. Evensen. 2003. An ensemble Kalman filter with a complex marine ecosystem model: hindcasting phytoplankton in the Cretan Sea. Ann. Geophys., *21*, 399–411.

Anderson, L. A., A. R. Robinson and C. J. Lozano. 2000. Physical and biological modeling in the Gulf Stream region: I. Data assimilation methodology. Deep-Sea Res. I, *47*, 1787–1827.

Anderson, T. R. 1993. A spectrally averaged model of light penetration and photosynthesis. Limnol. Oceanogr., *38*, 1403–1419.

——— 2005. Plankton functional type modelling: running before we can walk? J. Plankton Res., *27*, 1073–1081.

Armstrong, R. A., J. L. Sarmiento and R.D. Slater. 1995. Monitoring ocean productivity by assimilating satellite chlorophyll into ecosystem models, *in* Ecological Time Series, T. M. Powell and J. H. Steele, eds., Chapman and Hall, New York, 371–390.

Aumont, O., E. Maier-Reimer, S. Blain and P. Monfray. 2003. An ecosystem model of the global ocean including Fe, Si, P colimitations. Global Biogeochem. Cy., *17*, GB1060, doi:10.1029/2001GB001745.

Behrenfeld, M. J., E. Boss, D. A. Siegel and D. M. Shea. 2005. Carbon-based ocean productivity and phytoplankton physiology from space. Global Biogeochem. Cy., *19*, GB1006, doi:10.1029/2004GB002299.

Bell, M. J., R. M. Forbes and A. Hines. 2000. Assessment of the FOAM global data assimilation system for real-time operational ocean forecasting. J. Mar. Syst., *25*, 1–22.

Beşiktepe, Ş. T., P. F. J. Lermusiaux and A. R. Robinson. 2003. Coupled physical and biogeochemical data-driven simulations of Massachusetts Bay in late summer: real-time and postcruise data assimilation. J. Mar. Syst., *40–41*, 171–212.

Brasseur, P., P. Bahurel, L. Bertino, F. Birol, J. M. Brankart, N. Ferry, S. Losa, E. Remy, J. Schröter, S. Skachko, C. E. Testut, B. Tranchant, P. J. van Leeuwen and J. Verron. 2005. Data assimilation for marine monitoring and prediction: The MERCATOR operational assimilation systems and the MERSEA developments. Q. J. R. Roy. Meteor. Soc., *131*, 3561–3582.

Carmillet, V., J.-M. Brankart, P. Brasseur, H. Drange, G. Evensen and J. Verron. 2001. A singular evolutive extended Kalman filter to assimilate ocean color data in a coupled physical-biogeochemical model of the North Atlantic Ocean. Ocean Model., *3*, 167–192.

Conkright, M. E., S. Levitus, and T. P. Boyer. 1994. World Ocean Atlas 1994, Volume 1: Nutrients. NOAA Atlas NESDIS 1, U.S. Department of Commerce, NOAA, NESDIS.

Dadou, I., G. Evans and V. Garçon. 2004. Using JGOFS *in situ* and ocean color data to compare biogeochemical models and estimate their parameters in the subtropical North Atlantic Ocean. J. Mar. Res., *62*, 565–594.

Dowd, M. 2006. A sequential Monte Carlo approach for marine ecological prediction. Environmetrics, *17*, 435–455.

Eknes, M. and G. Evensen. 2002. An ensemble Kalman filter with a 1-D marine ecosystem model. J. Mar. Syst., *36*, 75–100.

Fasham, M. J. R., P. W. Boyd and G. Savidge. 1999. Modeling the relative contributions of autotrophs and heterotrophs to carbon flow at a lagrangian JGOFS station in the Northeast Atlantic: The importance of DOC. Limnol. Oceanogr., *44*, 80–94.

Fasham, M. J. R. and G. T. Evans. 1995. The use of optimization techniques to model marine ecosystem dynamics at the JGOFS station at 47°N 20°W. Philos. T. Roy. Soc. B, *348*, 203–209.

Fasham, M. J. R., K. J. Flynn, P. Pondaven, T. R. Anderson and P. W. Boyd. 2006. Development of a robust marine ecosystem model to predict the role of iron in biogeochemical cycles: A comparison of results for iron-replete and iron-limited areas, and the SOIREE iron-enrichment experiment. Deep-Sea Res. I, *53*, 333–366.

Faugeras, B., O. Bernard, A. Sciandra and M. Lévy. 2004. A mechanistic modelling and data assimilation approach to estimate the carbon/chlorophyll and carbon/nitrogen ratios in a coupled hydrodynamical-biological model. Nonlinear Proc. Geoph., *11*, 515–533.

Faugeras, B., M. Lévy, L. Mémery, J. Verron, J. Blum and I. Charpentier. 2003. Can biogeochemical fluxes be recovered from nitrate and chlorophyll data? A case study assimilating data in the Northwestern Mediterranean Sea at the JGOFS-DYFAMED station. J. Mar. Syst., *40–41*, 99–125.

Fennel, K., M. Losch, J. Schröter and M. Wenzel. 2001. Testing a marine ecosystem model: sensitivity analysis and parameter optimization. J. Mar. Syst., *28*, 45–63.

Friedrichs, M. A. M. 2002. Assimilation of JGOFS EqPac and SeaWiFS data into a marine ecosystem model of the central equatorial Pacific Ocean. Deep-Sea Res. II, *49*, 289–319.

Friedrichs, M. A. M., R. R. Hood and J. D. Wiggert. 2006. Ecosystem model complexity versus physical forcing: Quantification of their relative impact with assimilated Arabian Sea data. Deep-Sea Res. II, *53*, 576–600.

Garcia-Gorriz, E., N. Hoepffner and M. Ouberdous. 2003. Assimilation of SeaWiFS data in a coupled physical-biological model of the Adriatic Sea. J. Mar. Syst., *40–41*, 233–252.

Geider, R. J., H. L. MacIntyre and T. M. Kana. 1997. Dynamic model of phytoplankton growth and acclimation: Responses of the balanced growth rate and the chlorophyll *a*:carbon ratio to light, nutrient-limitation and temperature. Mar. Ecol. Prog. Ser., *148*, 187–200.

Gregg, W. W. 2007. Assimilation of SeaWiFS ocean chlorophyll data into a three-dimensional global ocean model. J. Mar. Syst., doi:10.1016/j.jmarsys.2006.02.015.

Gregg, W. W., P. Ginoux, P. S. Schopf and N. W. Casey. 2003. Phytoplankton and iron: validation of a global three-dimensional ocean biogeochemical model. Deep-Sea Res. II, *50*, 3143–3169.

Hemmings, J. C. P., M. A. Srokosz, P. Challenor and M. J. R. Fasham. 2003. Assimilating satellite ocean-colour observations into oceanic ecosystem models. Philos. T. Roy. Soc. A, *361*, 33–39.

——— 2004. Split-domain calibration of an ecosystem model using satellite ocean colour data. J. Mar. Syst., *50*, 141-179.

Hoteit, I., G. Triantafyllou, G. Petihakis and J. I. Allen. 2003. A singular evolutive extended Kalman filter to assimilate real *in situ* data in a 1-D marine ecosystem model. Ann. Geophys., *21*, 389–397.

Hoteit, I., G. Triantafyllou and G. Petihakis. 2005. Efficient data assimilation into a complex, 3-D physical-biogeochemical model using partially-local Kalman filters. Ann. Geophys., *23*, 3171–3185.

Huret, M., F. Gohin, D. Delmas, Michel Lunven and V. Garçon. 2007. Use of SeaWiFS data for light availability and parameter estimation of a phytoplankton production model of the Bay of Biscay. J. Mar. Syst., *65*, 509–531.

Hurtt, G. C. and R. A. Armstrong. 1996. A pelagic ecosystem model calibrated with BATS data. Deep-Sea Res. II, *43*, 653–683.

——— 1999. A pelagic ecosystem model calibrated with BATS and OWSI data. Deep-Sea Res. I, *46*, 27–61.

Ishizaka, J. 1990. Coupling of Coastal Zone Color Scanner data to a physical-biological model of the southeastern united-states continental-shelf ecosystem. 3. Nutrient and phytoplankton fluxes and CZCS data assimilation. J. Geophys. Res. Oceans, *95*, 20201–20212.

Kuroda, H. and M. J. Kishi. 2004. A data assimilation technique applied to estimate parameters for the NEMURO marine ecosystem model. Ecol. Model., *172*, 69–85.

Lenartz, F., C. Raick, K. Soetaert and M. Grégoire. 2007. Application of an ensemble Kalman filter to a 1-D coupled hydrodynamic-ecosystem model of the Ligurian Sea. J. Mar. Syst., doi:10.1016/j.jmarsys.2006.12.001.

Losa, S. N., G. A. Kivman and V. A. Ryabchenko. 2004. Weak constraint parameter estimation for a simple ocean ecosystem model: what can we learn about the model and data? J. Mar. Syst., *45*, 1–20.

Losa, S. N., G. A. Kivman, J. Schröter and M. Wenzel. 2003. Sequential weak constraint parameter estimation in an ecosystem model. J. Mar. Syst., *43*, 31–49.

Losa, S. N., A. Vézina, D. Wright, Y. Y. Lu, K. Thompson and M. Dowd. 2006. 3D ecosystem modelling in the North Atlantic: Relative impacts of physical and biological parameterizations. J. Mar. Syst., *61*, 230–245.

Magri, S., P. Brasseur and G. Lacroix. 2005. Data assimilation in a marine ecosystem model of the Ligurian Sea. C. R. Geosci., *337*, 1065–1074.

Matear, R. J. 1995. Parameter optimization and analysis of ecosystem models using simulated annealing: A case study at Station P. J. Mar. Res., *53*, 571–607.

Moore, J. K., S. C. Doney and K. Lindsay. 2004. Upper ocean ecosystem dynamics and iron cycling in a global three-dimensional model. Global Biogeochem. Cy., *18*, GB4028, doi:10.1029/2004GB002220.

Natvik, L.-J. and G. Evensen. 2003. Assimilation of ocean colour data into a biochemical model of the North Atlantic: Part 1. Data assimilation experiments. J. Mar. Syst., *40–41*, 127–153.

Nerger, L. and W. W. Gregg. 2007a. Assimilation of SeaWiFS data into a global ocean-biogeochemical model using a local SEIK filter. J. Mar. Syst., *68*, 237–254.

—— 2007b. Improving assimilation of SeaWiFS data by the application of bias correction with a local SEIK filter. J. Mar. Syst., doi:10.1016/j.jmarsys.2007.09.07.

Oschlies, A. and M. Schartau. 2005. Basin-scale performance of a locally optimized marine ecosystem model. J. Mar. Res., *63*, 335–358.

Palmer, J. R. and I. J. Totterdell. 2001. Production and export in a global ocean ecosystem model. Deep-Sea Res. I, *48*, 1169–1198.

Park, S. K. and A. Zupanski. 2003. Four-dimensional variational data assimilation for mesoscale and storm-scale applications. Meteorol. Atmos. Phys., *82*, 173–208.

Popova, E. E., C. J. Lozano, M. A. Srokosz, M. J. R. Fasham, P. J. Haley and A. R. Robinson. 2002a. Coupled 3D physical and biological modelling of the mesoscale variability observed in North-East Atlantic in spring 1997: biological processes. Deep-Sea Res. I, *49*, 1741–1768.

Popova, E. E., M. A. Srokosz and D. A. Smeed. 2002b. Real-time forecasting of biological and physical dynamics at the Iceland-Faeroes Front in June 2001. Geophys. Res. Lett., *29*:doi:10.1029/2001GL013706.

Prunet, P., J. F. Minster, D. Ruiz-Pino and I. Dadou. 1996a. Assimilation of surface data in a one-dimensional physical-biogeochemical model of the surface ocean. 1. Method and preliminary results. Global Biogeochem. Cy., *10*, 111–138.

Prunet, P., J. F. Minster, V. Echevin and I. Dadou. 1996b. Assimilation of surface data in a one-dimensional physical-biogeochemical model of the surface ocean. 2. Adjusting a simple trophic model to chlorophyll, temperature, nitrate, and pCO_2 data. Global Biogeochem. Cy., *10*, 139–158.

Raick, C., A. Alvera-Azcarate, A. Barth, J. M. Brankart, K. Soetaert and M. Grégoire, 2007. Application of a SEEK filter to a 1D biogeochemical model of the Ligurian Sea: Twin experiments and real *in-situ* data assimilation. J. Mar. Syst., *65*, 561–583.

Schartau, M., A. Oschlies and J. Willebrand. 2001. Parameter estimates of a zero-dimensional ecosystem model applying the adjoint method. Deep-Sea Res. II, *48*, 1769–1800.

Schartau, M. and A. Oschlies. 2003a. Simultaneous data-based optimization of a 1D-ecosystem model at three locations in the North Atlantic: Part I – Method and parameter estimates. J. Mar. Res., *61*, 765–793.

Schartau, M. and A. Oschlies. 2003b. Simultaneous data-based optimization of a 1D-ecosystem model at three locations in the North Atlantic: Part II – Standing stocks and nitrogen fluxes. J. Mar. Res., *61*, 795–821.

Six, K. D. and E. Maier-Reimer. 1996. Effects of plankton dynamics on seasonal carbon fluxes in an ocean general circulation model. Global Biogeochem. Cy., *10*, 559–583.

Spitz, Y. H., J. R. Moisan, M. R. Abbott and J. G. Richman. 1998. Data assimilation and a pelagic ecosystem model: parameterization using time series observations. J. Mar. Syst., *16*, 51–68.

Spitz, Y. H., J. R. Moisan and M. R. Abbott. 2001. Configuring an ecosystem model using data from the Bermuda Atlantic Time Series (BATS). Deep-Sea Res. II, *48*, 1733–1768.

Tjiputra, J. F., D. Polzin and A. M. E. Winguth. 2007. Assimilation of seasonal chlorophyll and nutrient data into an adjoint three-dimensional ocean carbon cycle model: sensitivity analysis and ecosystem parameter optimization. Global Biogeochem. Cy., *21*, GB1001, doi:10.1029/2006GB002745.

Torres, R., J. I. Allen and F. G. Figueiras. 2006. Sequential data assimilation in an upwelling influenced estuary. J. Mar. Syst., *60*, 317–329.

Weber, L., C. Volker, M. Schartau and D. A. Wolf-Gladrow. 2005. Modeling the speciation and biogeochemistry of iron at the Bermuda Atlantic Time-series Study site. Global Biogeochem. Cy., *19*, GB1019, doi:10.1029/2004GB002340.

Received: *24 May, 2007*; revised: *6 February, 2008*.